



Materials and metals in MSR

Presented by Victor Ignatiev

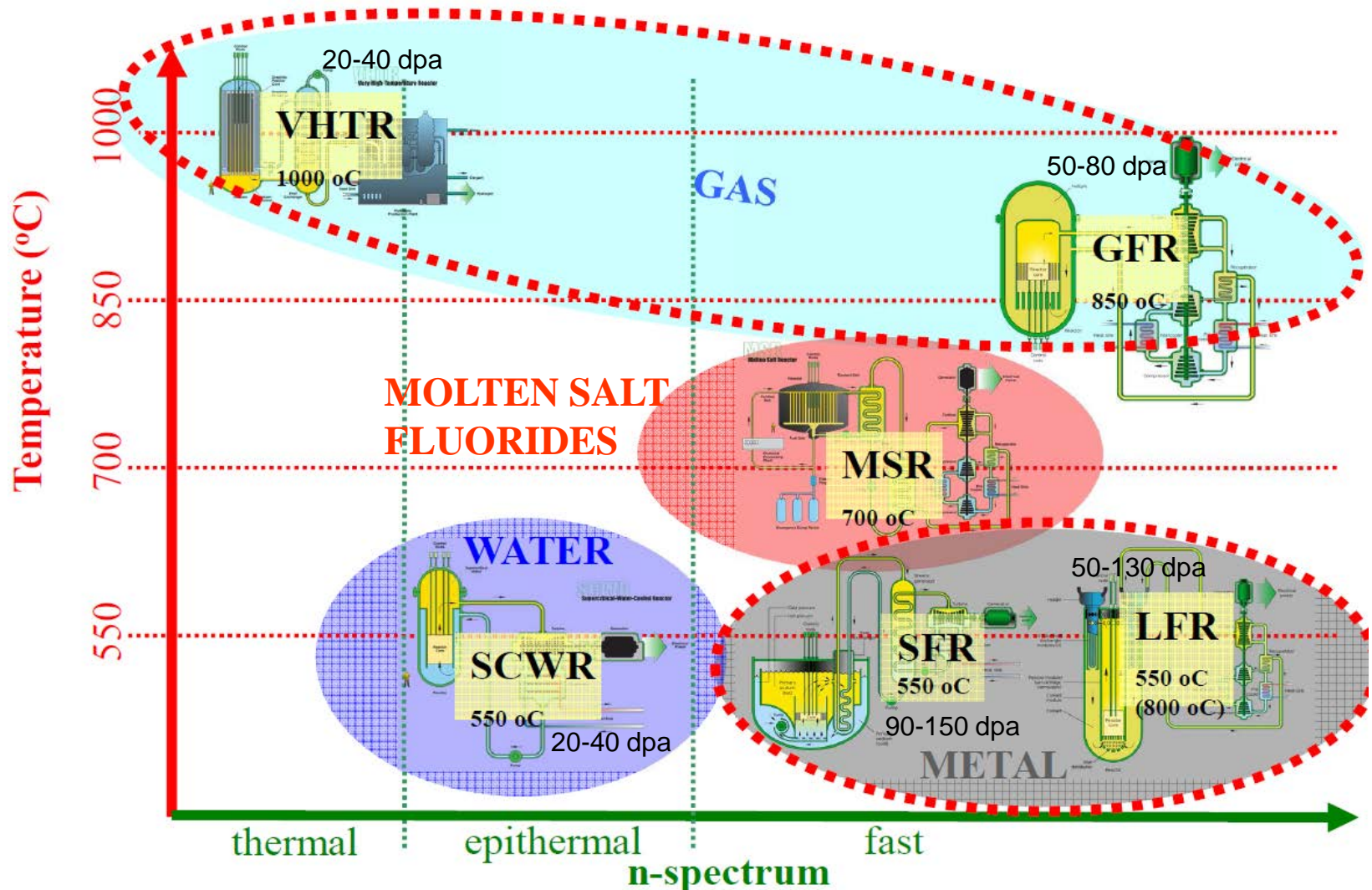
National Research Center “Kurchatov Institute”

123182, Kurchatov sq., 1, Moscow, Russia

Ignatiev_VV@nrcki.ru



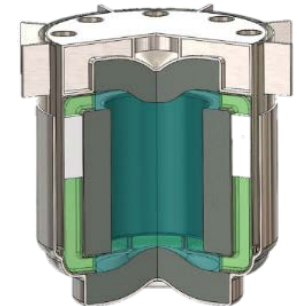
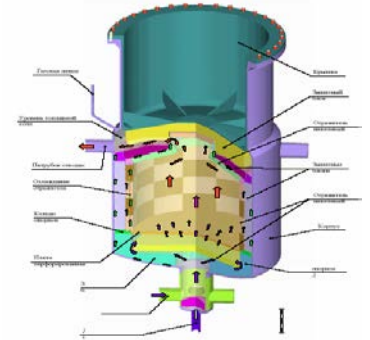
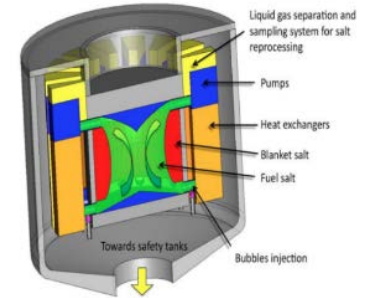
All GEN IV reactors require higher operating temperatures and / or radiation doses. The higher operating temperatures / dose rate require materials increased high temperature strength, thermal stability and irradiation resistance.





Different Reactor Concepts using Molten Salt are Discussed at GIF MSR pSSC Meetings

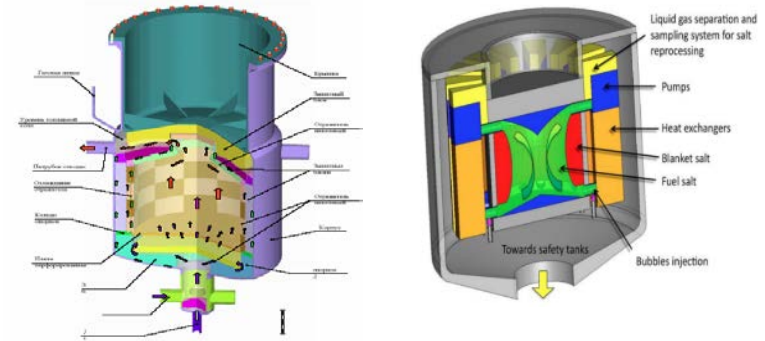
- Within the GIF, research is performed on the MSR concepts, under the MOU signed by Euratom, France, the Russian Federation, Switzerland and USA. China, Australia, Korea, Japan and contribute as observers.
- Two fast spectrum MSR concepts are being studied, large power units based on homogeneous core with liquid fluoride-salt circulating fuel: MSFR design in France, Euratom and Switzerland as well as MOSART concept in the Russian Federation. R&D studies are on-going in order to verify that fast spectrum MSR systems satisfy the goals of Gen-IV reactors in terms of sustainability, non-proliferation, safety and waste management.
- The US is working on solid fuel FHR (Fluoride-salt-cooled High-temperature Reactor) as well as liquid fueled MCFR (Molten Chloride salt Fast Reactor)
- China, as observer in the pSSC of the MSR, is working on FHR and TMSR (Thorium Molten fluoride Salt thermal Reactor) graphite moderated designs.





Introduction

Fuel circuit	MOSART	MSFR
Fuel salt, mole%	LiF-BeF ₂ +1TRUF ₃ LiF- BeF ₂ +5ThF ₄ +1UF ₄ +1TRUF ₃	78.6LiF-12.9ThF ₄ - 3.5UF ₄ - 5TRUF ₃ 77.5LiF-6.6ThF ₄ - 12.3UF ₄ -3.6TRUF ₃
Temperature, °C	620 - 720	650 - 750
Core radius/height, m	1.4 / 2.8	1.13 / 2.26
Core specific power, W/cm ³	130	330
Container material	Ni-Mo alloy	Ni-W alloy



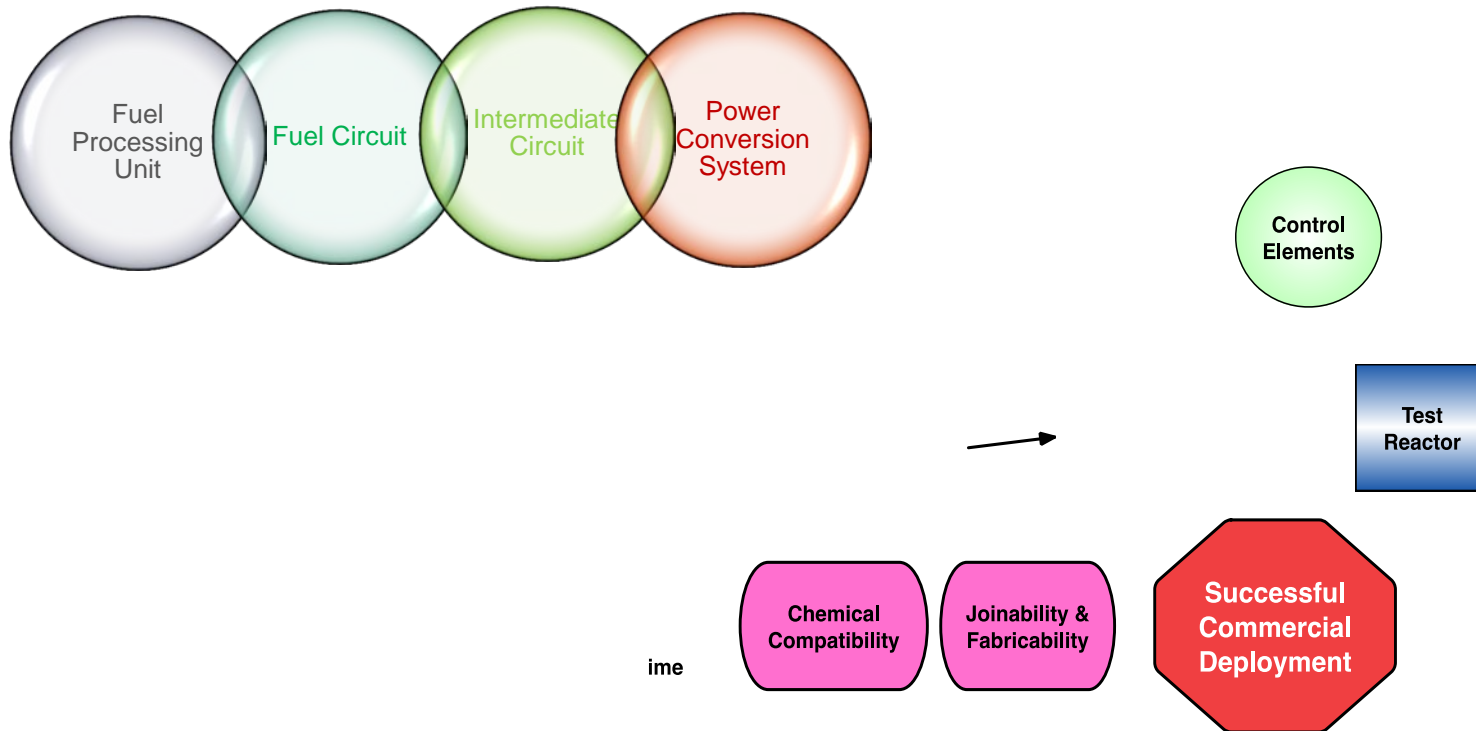
- Present MSR concepts with homogeneous core utilizes Ni-base alloy as the containment vessel and other metallic parts of the system, probably graphite as reflector, and a liquid fluoride salt containing LiF, (BeF₂), UF₄, TRUF₃ and ThF₄ as the fertile-fissile medium.
- The fertile-fissile salt will leave the reactor vessel at a temperatures > 700°C and energy will be transferred to a coolant salt which in turn is used to produce supercritical steam.

Element	Time	Method
Kr, Xe	50 s	Sparging with He
Zn, Ga, Ge, As, Se, Nb, Mo, Ru, Rh, Pd, Ag, Tc, Cd, In, Sn, Sb, Te	2-4 hrs	Partial plating on surfaces, removal to off-gas system, limited filtering
²³³ U, ²³⁴ U, ²³⁵ U, ²³⁶ U, ²³⁷ U	10 days	Fluorination
Zr, ²³³ Pa	1-3 yrs	Reductive extraction in liquid Bi
Ni, Fe, Cr	1-3 yrs	
Pu, Am, Cm, Np	1-3 yrs	
Y, La, Ce, Pr, Nd, Pm, Gd, Tb, Dy, Ho, Er	1-3 yrs	
Sm, Eu	1-3 yrs	
Sr, Ba, Rb, Cs	5-10 yrs	
Li, Be, Th	30 yrs	Salt discard



MSR Commercial Deployment Depends Upon Resolving Multiple Materials Issues

Boundaries and Interfaces





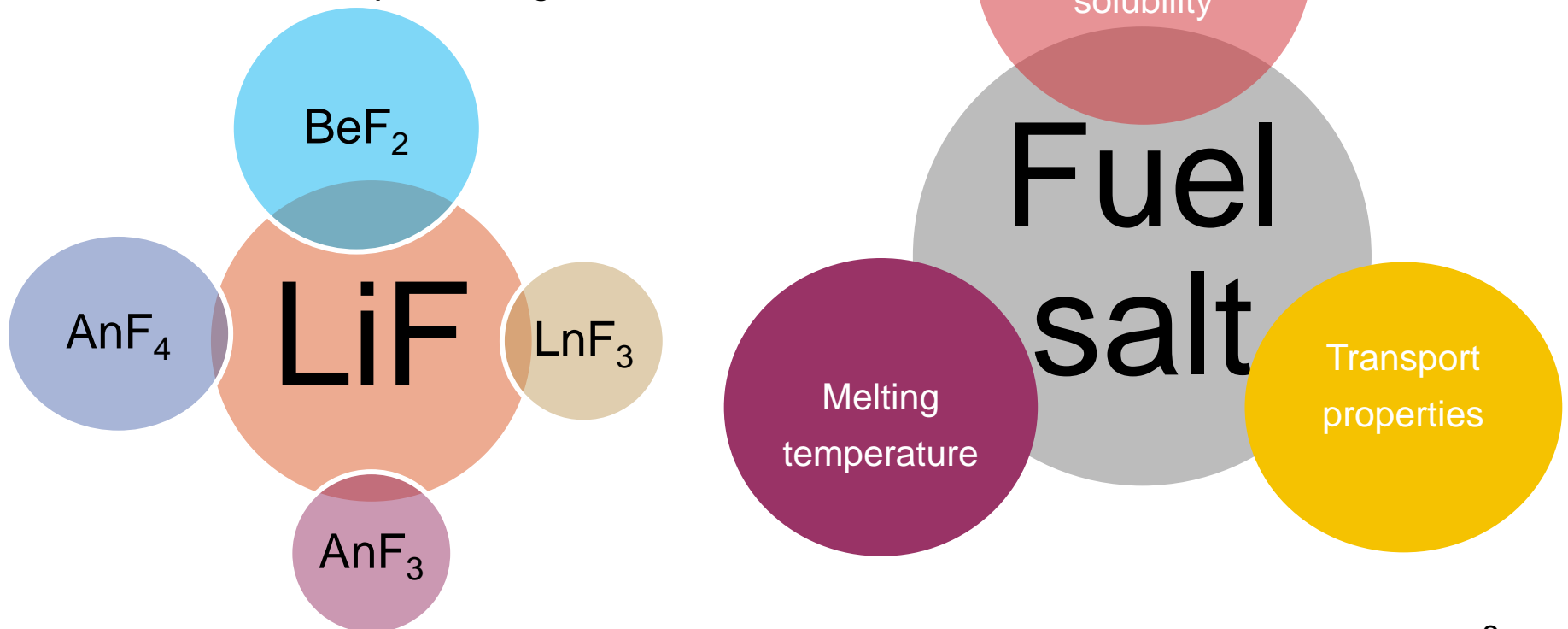
MSRs Have Several Remaining Technology Challenges

- ✓ *Operating experience with the MSRE has demonstrated the excellent compatibility of the “graphite - Hastelloy N - fluoride salt” system at 650°C.*
- ✓ *Several improvements in materials are needed for MSR with a basic plant life of 40 years; specifically:*
 - High temperature (720°C and 750°C) and high critical concentrations of actinides fluorides in primary circuit; Ni-based alloy with improved resistance to embrittlement by fast ($<10^{21}$ n/cm²) and thermal (6×10^{21} n/cm²) neutrons; probably, graphite with better dimensional stability in a fast neutron flux; graphite that is sealed to obtain a surface permeability of $<10^{-8}$ cm²/s; secondary coolant that is inexpensive and has a melting point of 400° C; materials be compatible with all environments in the processing plant.
 - Proper chemistry control is imperative
 - Ratio of U⁴⁺/ U³⁺ is key to maintaining low corrosivity, including Te IGC
 - Molten salts can generate substantial amounts of tritium
 - Especially lithium bearing salts (e.g. ${}^6\text{LiF} + n \rightarrow {}_2^4\text{He} + {}_1^3\text{HF}$)
 - Tritium control and corrosion control can't be separate



In most cases the base-line fuel / coolant salt is lithium-beryllium fluoride salt as it has best properties

- *Low neutron cross section for the solvent*
- *Thermal stability of the salt components*
- *Low vapor pressure*
- *Radiation stability*
- *Adequate solubility of fuel and FP's components*
- *Adequate transport properties*
- *Compatibility with construction materials*
- *Low fuel and processing costs*





Preparative Chemistry and Salt Purification

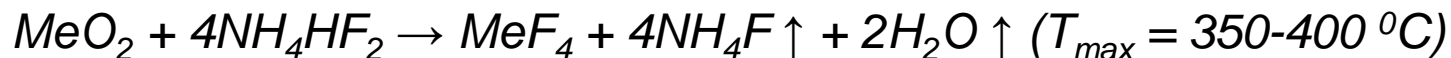
Most suppliers of halide salts do not provide materials that can be used directly

The major impurities that must be removed to prevent severe corrosion of the container metal are moisture/oxide contaminants

Once removed, these salts must be kept from atmospheric contamination by handling and storage in sealed containers

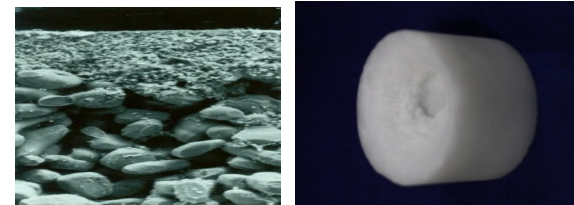
During the US MSR program, a considerable effort was devoted to salt purification by HF/H₂ sparging of the molten salt. In addition to removing moisture/oxide impurities, the purification also removes other halide contaminants, such as chloride and sulfur.

- *In our purifications the gaseous agent (HF) was in some cases replaced by solid ammonium hydrofluoride (NH₄HF₂, T_m ≈ 125 °C), which is safer and more convenient in use for the removal of impurity oxide compounds from metal fluorides and for the conversion of U and Th oxides to fluorides.*



- *To carry out these processes do not require expensive equipment and special safety measures. The purified anhydrous fluorides of metals was obtained, which are used for the preparation of fluoride salt melts of different composition.*

Production of anhydrous constituents -> Melting -> Filtration -> Zone recrystallization -> met. Th or Zr or Be treatment

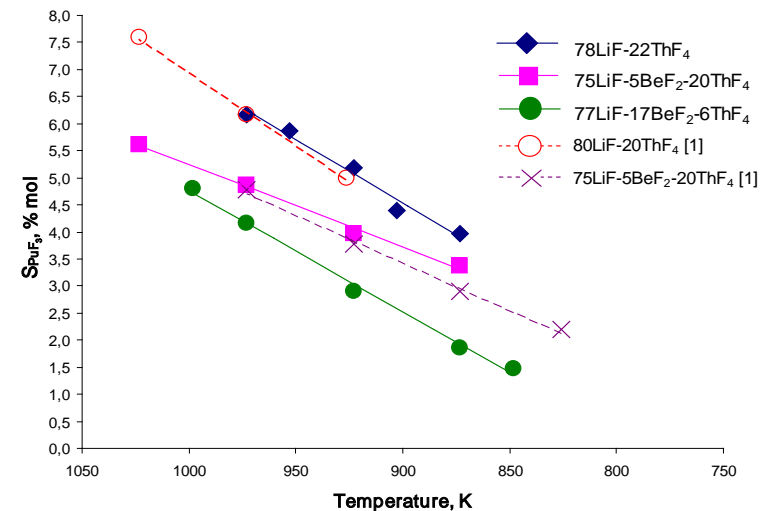
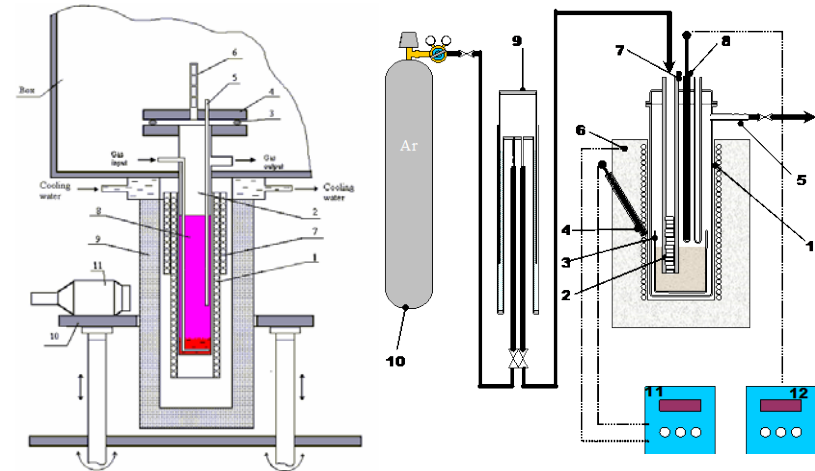




The data on PuF_3 solubility in molten salt fluorides appear to follow a linear relationship within the experimental accuracy of the measurements when plotted as \log of molar concentration of AnF_3 vs. $1/T(\text{K})$

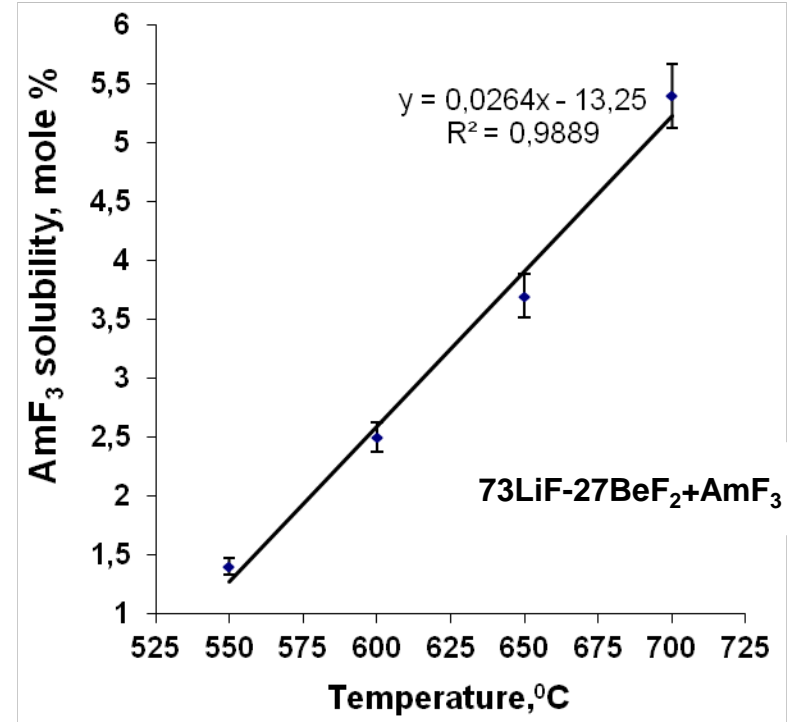
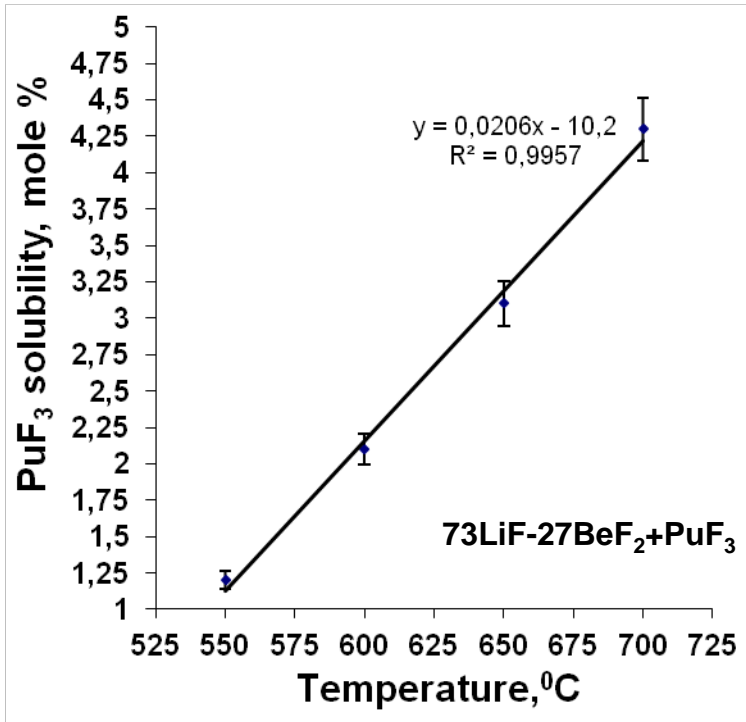
LiF	NaF	KF	BeF_2	ThF_4	T, K	A	$-B \cdot 10^{-3}$
46.5	11.5	42	0	0	823-973	5.59	3.949
73	0	0	27	0	825-1000	3.927	3.099
66	0	0	34	0	800-900	3.231	3.096
15	58	0	27	0	825-925	3.639	2.750
17	58	0	25	0	800-900	3.253	2.578
78	0	0	0	22	873-973	2.58	1.73
75	0	0	5	20	873-1023	2.06	1.34
77	0	0	17	6	848-998	3.61	2.91

$$\log S_{\text{PuF}_3}, \text{mol}\% = A + B/T, \text{K}$$





An and Ln Trifluoride Solubility



Temperature, K	72,5LiF-7ThF ₄ -20,5UF ₄		78LiF-7ThF ₄ -15UF ₄	
	PuF ₃	CeF ₃	PuF ₃	CeF ₃
873	0,35±0,02	1,5±0,1	1,45±0,7	2,6±0,1
923	4,5±0,2	2,5±0,1	5,6±0,3	3,6±0,2
973	8,4±0,4	3,7±0,2	9,5±0,5	4,8±0,3
1023	9,4±0,5	3,9±0,2	10,5±0,6	5,0±0,3

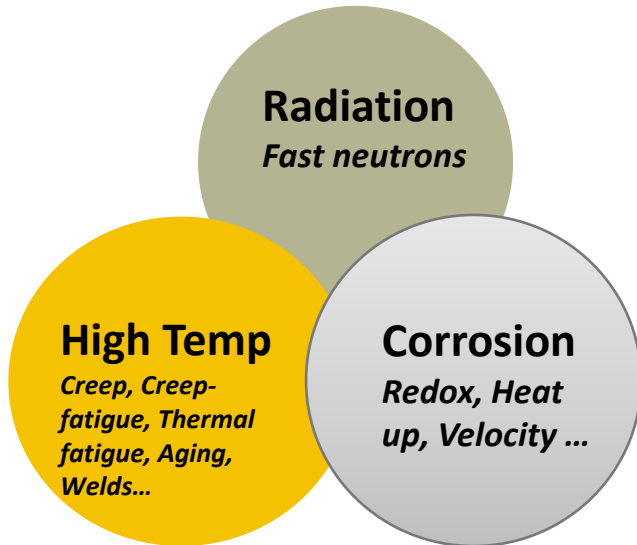
Near the liquids temperature for 78LiF-7ThF₄-15UF₄ and 72,5LiF-7ThF₄-20,5UF₄ salts, the CeF₃ significantly displace PuF₃



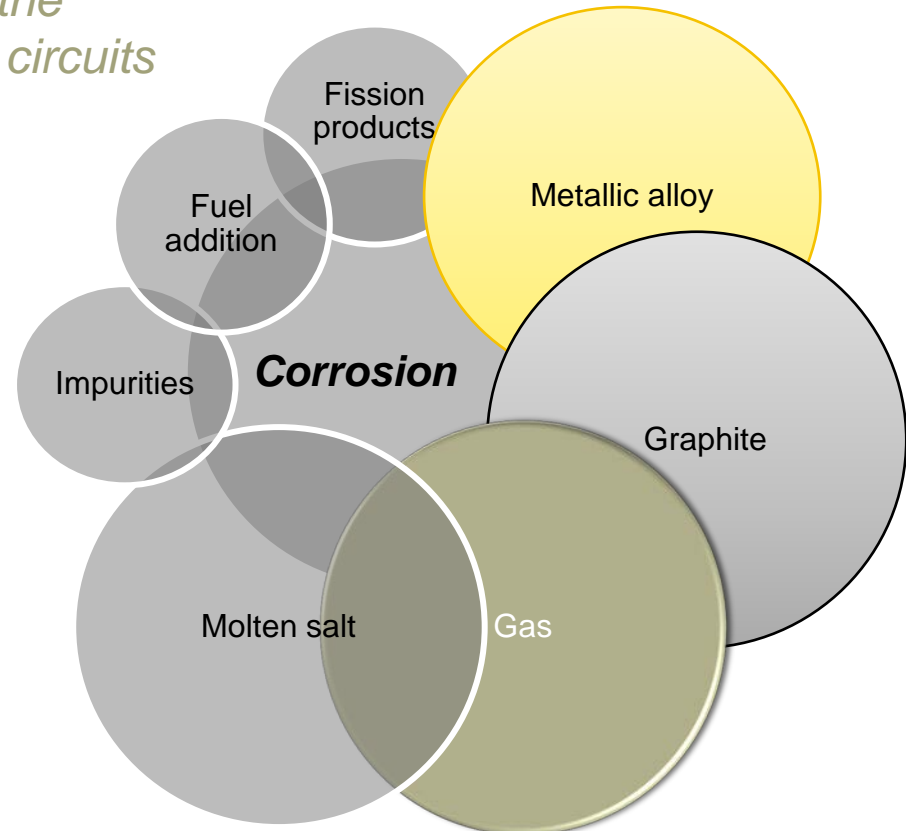
Gen IV MSR Container Materials

The success of MSR is strongly dependent on the compatibility of the container materials with the molten salts used in primary and secondary circuits

Combined environments



Corrosion effects

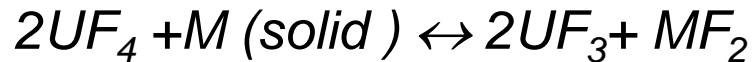


Because the products of oxidation of metals by fluoride melts are quite soluble in corroding media, passivation is precluded, and the corrosion rate depends on other factors, including: Oxidants, Thermal gradients, Salt flow rate, Galvanic coupling



Container metal for 1st and 2nd circuits in MSR

- Thermodynamic data reveal that in reactions with structural metals (M):



- Chromium is much more readily attacked than Fe, Ni, or Mo
- Stainless steels, having more Cr than Ni-based alloy Hastelloy N, are more susceptible to corrosion by fluoride melts

Oxidation and selective attack may also result from impurities in the melt:

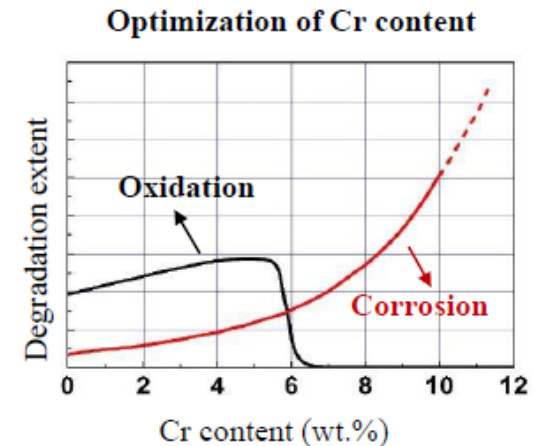
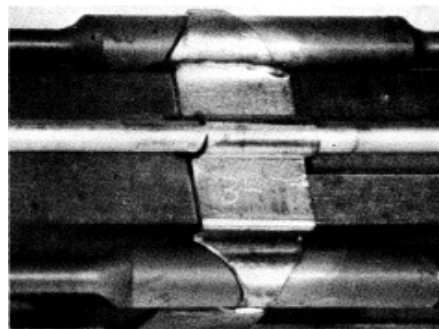


or oxide films on the metal:



followed by reaction of NiF_2 with M

Graphite and Hastelloy-N surveillance assembly removed from MSRE





The development of the GEN IV MSR concepts required a creating alloys of increased heat resistance, radiation and corrosion-mechanical durability when operating at temperatures up to 800 °C. The nickel based alloys with improved corrosion-mechanical properties were developed in Russia (HN80M-VI, HN80MTY, HN80MTW), Czech Republic (MONICR) , France (EM-721, EM-722) and China (G3535).

Element	Hasteloy N US	Hasteloy NM US	Hasteloy-N UNS10003 US	Hastelloy -NM, 1976	HN80-MT Russia	HN80M-VI Russia	HN80MTY (EK-50) Russia	HN80M TW Russia	MONICR Czech Rep	GH3535 China	EM-721 France
Ni	base	base	base	base	base	82	82	77	base	base	68.8
Cr	7.52	7.3	7	6-8	7.02	7.61	6,81	7	6,85	7.0	5.7
Mo	16.28	13.6	16	11-13	12.1	12.2	13,2	10	15,8	17.3	0.07
Ti	0.26	0.5–2.0	Ti+Al= 0.5	-	1.72	0.001	0,93	1.7	0,026	0.002	0.13
Al	0.26	-		-	-	0.038	1,12	-	0,02	0.021	0.08
Fe	3.97	< 0.1	4.0 max	0.1	< 0.33	0.28	0,15	< 0.33	2,27	3.9	<0.05
Mn	0.52	0.14	0.8 max	0.15-0.25	<0.1	0.22	0,013	<0.1	0,037	0.6	0.086
Nb	-	-	-	1 - 2	-	1.48	0,01	-	< 0,01	-	-
Si	0.5	< 0.01	0.5	0.1	<0.05	0.040	0,040	<0.05	0,13	0.45	0.065
W	0.06	-	-	-	-	0.21	0,072	6	0,16	-	25.2
Cu	0.02	-	0.35 max	-	<0.1	0.12	0.02	< 0.1	0.016	0.007	-
C	0.05	0.05	0.06 max	0.05	0.02	0.02	<0.025	<0.0032	0.014	0.055	<0.002

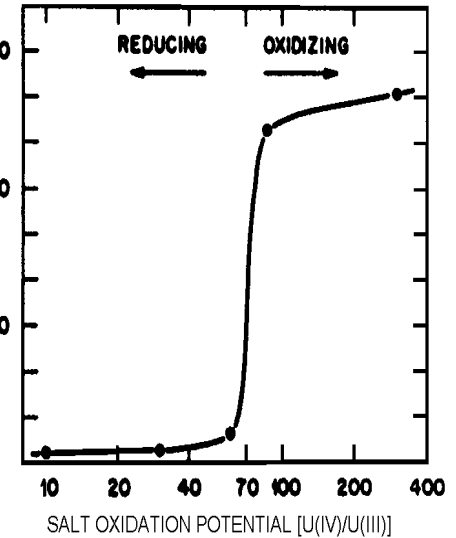
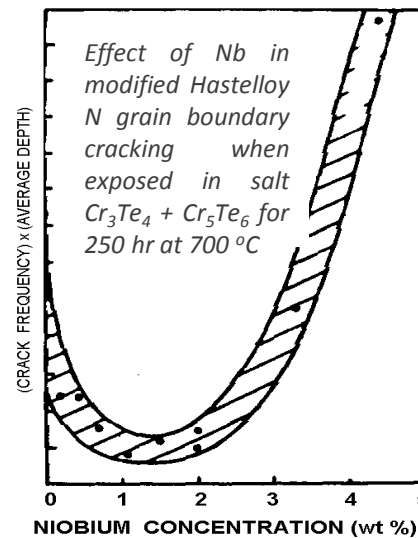
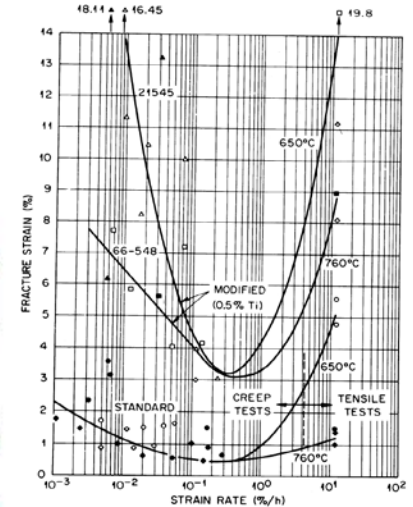
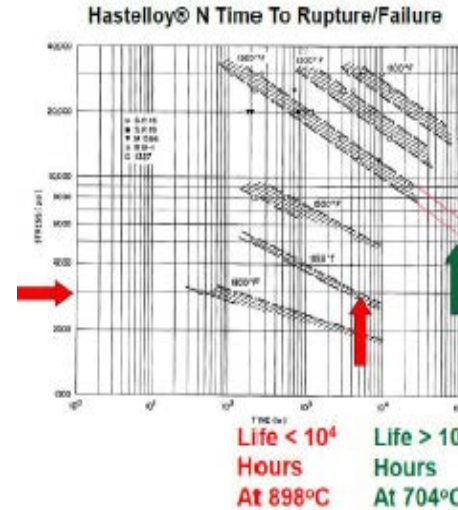


ORNL developments with Alloy N

- Hastelloy N was susceptible to damage from He formation in a fast neutron flux. Later it was found that modified alloys that had fine carbide precipitates within grains would hold He and restrain this migration to the grain boundaries. Several alloys have been prepared that retain good postirradiation properties after irradiation at 760°C.

- The reasoning in 1970's was that the 2% titanium addition would impart good resistance to irradiation embrittlement and that the 0 to 2% niobium addition would impart good resistance to intergranular tellurium embrittlement.

- Hastelloy N was deteriorating in its properties as a result of intergranular attack caused by Te. Later work showed that this Te attack could be controlled by keeping the fuel on the reducing side. This is done by adjustment of the chemistry so that: about 2%UF₃ as opposed to 98%UF₄



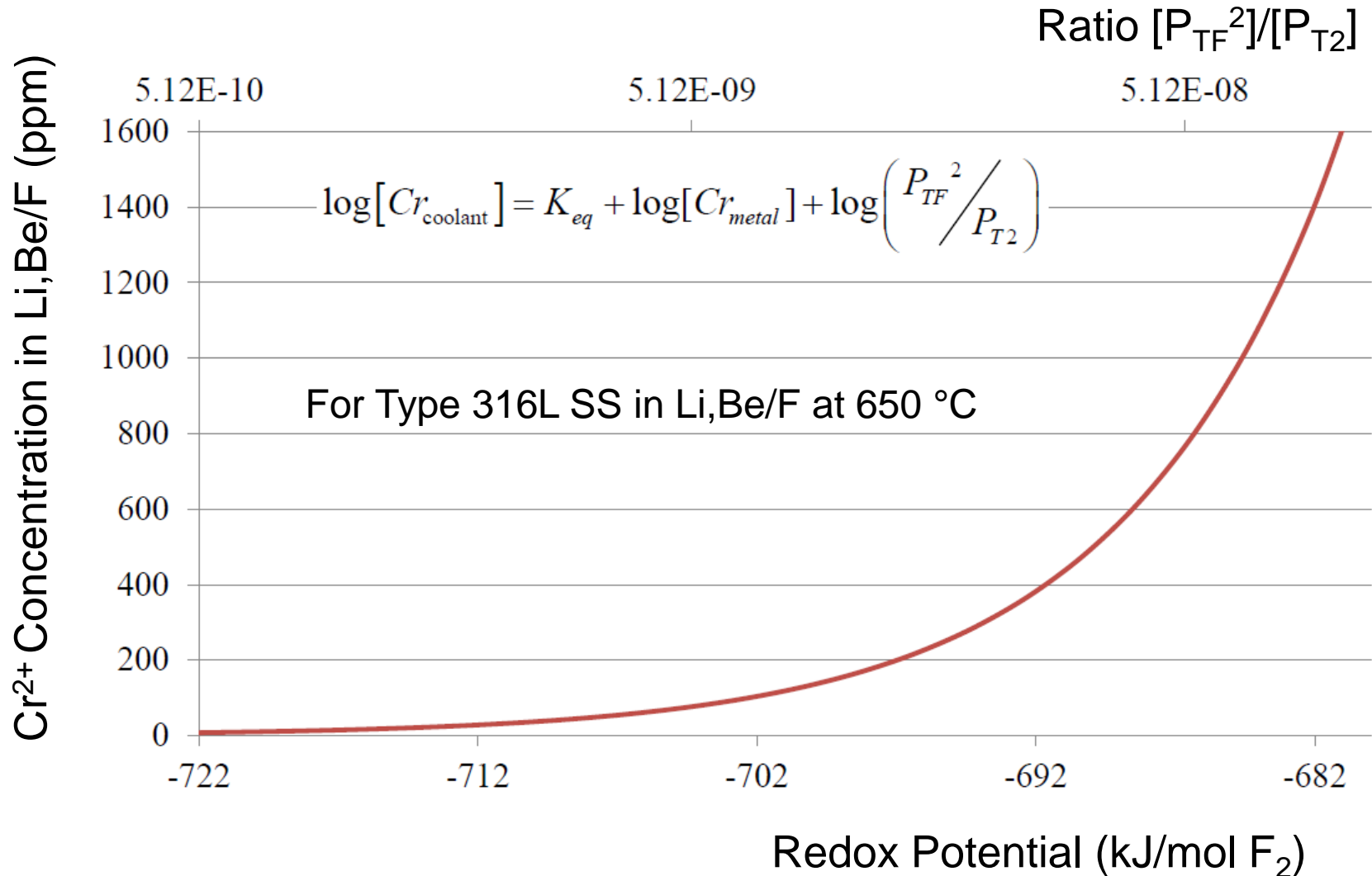


MSR Coolant Behavior

- The reaction of steam with Li_2BeF_4 yields HF and BeO
$$\text{H}_2\text{O}(\text{g}) + \text{BeF}_2(\text{P}) \rightarrow \text{BeO}(\text{c}) + 2\text{HF}(\text{g})$$
- Both H_2O and HF are likely to corrode the metal in contact with the salt; corrosion-product fluorides will dissolve or be otherwise carried by the salt. Since BeO is only very slightly soluble in Li_2BeF_4 , a large in-leakage of steam would soon lead to the precipitation of BeO in the salt circuit.
- Moisture in the air will also react, as does steam, with Li_2BeF_4 . The molten Li_2BeF_4 can, if necessary, be freed of oxide by treatment at elevated temperatures with anhydrous HF
- From Li_2BeF_4 , metallic Li, Na, or K react to precipitate Be metal, but the reaction is not highly exothermic.



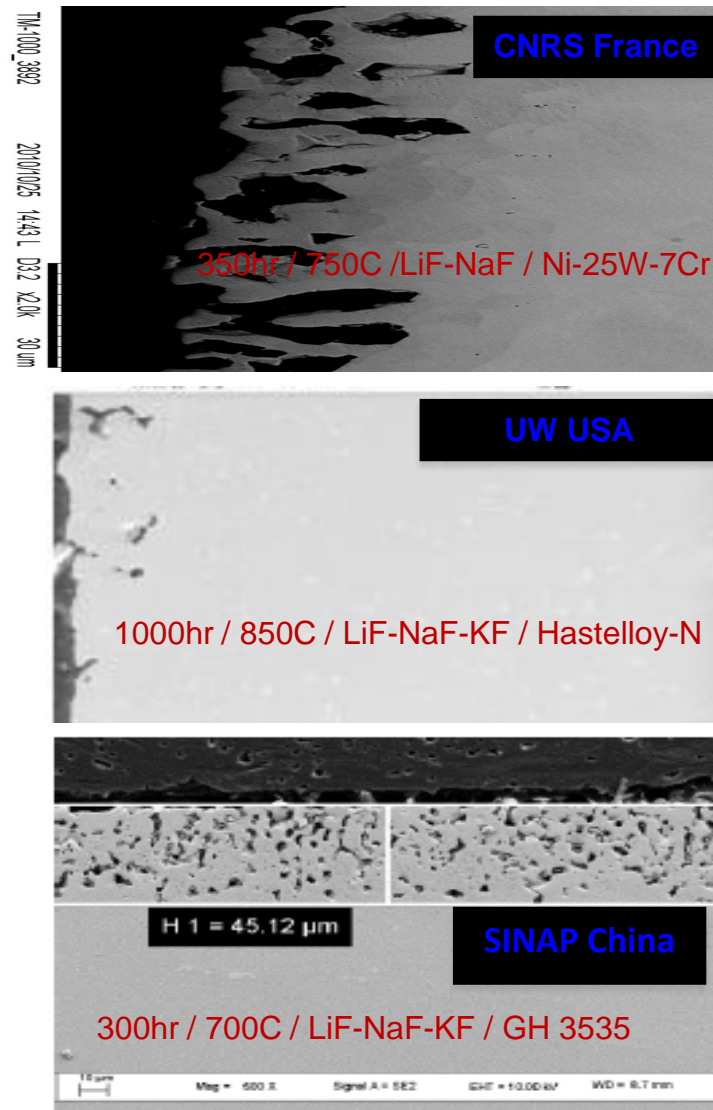
Redox Potential Determines Extent of Corrosion





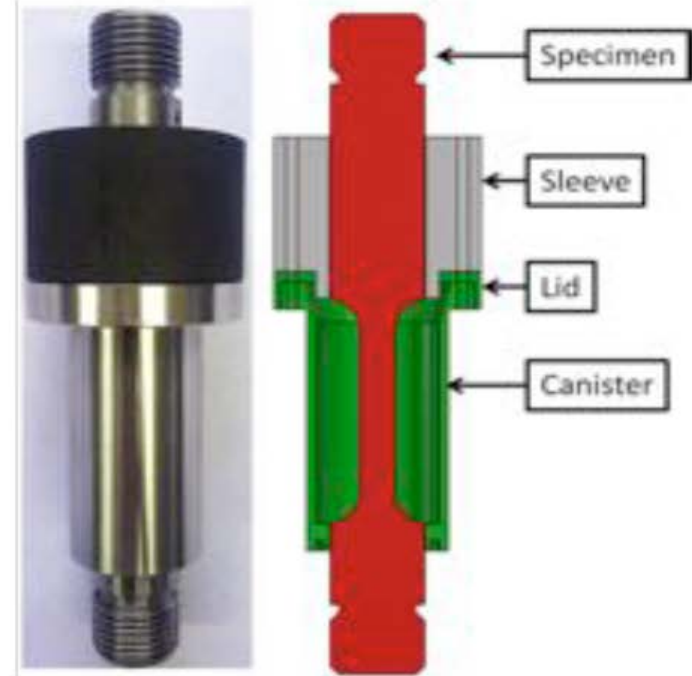
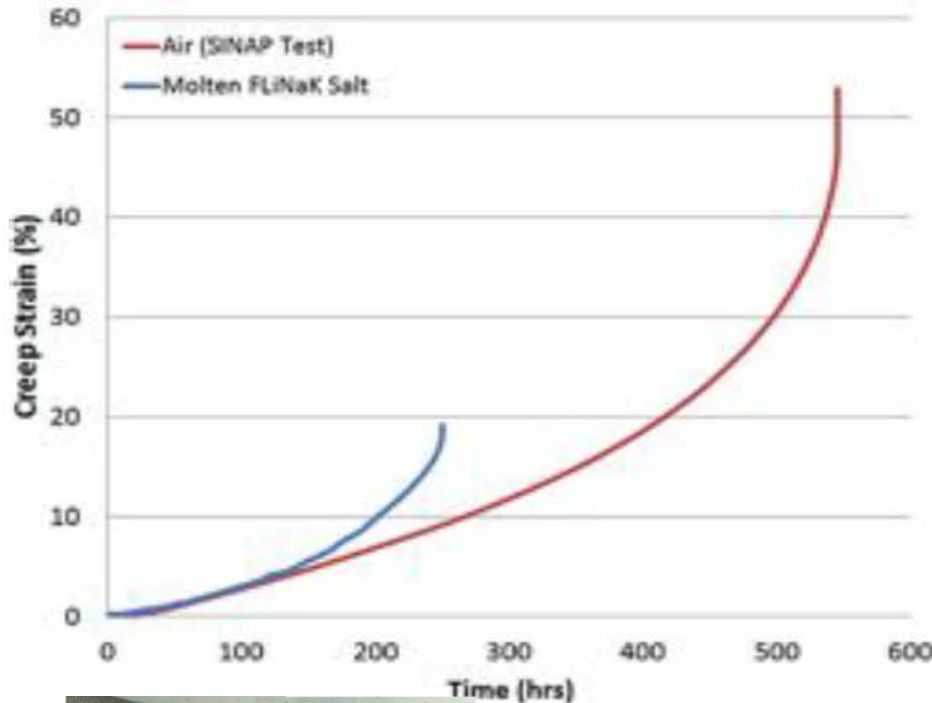
Corrosion in Li,Na,(K)/F

- Results reveal that the corrosion of Ni-based alloy is mainly induced by the dealloying of Cr.
- Cr dissolved in molten FLiNaK salt is in the form of Na_3CrF_6 . The dissolution of Cr and other elements result in the formation of voids in alloy. SO_4^{2-} and H_2O in molten FLiNaK salt can aggravate the corrosion of Ni-based alloy.
- Therefore, the corrosion rate of alloy can be controlled by the purification of FLiNaK salt. Results reveal that Ni-based alloy and the weld joint exhibit excellent corrosion resistance in the purified molten FLiNaK salt at 700°C .





Combined environments: Corrosion + High Temperature Creep



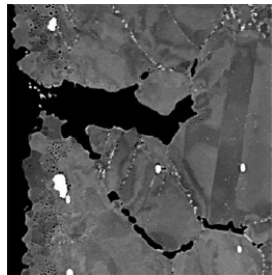
GH3535 creep rupture test (190 MPa, 700°C)
Results show significant effect of salt on creep life



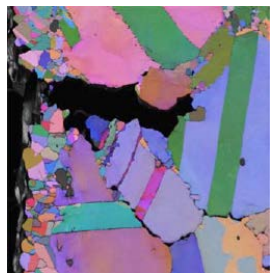
O. Muránsky, L. Edwards "Molten Salt Reactor (MSR) Research in Australia: High-Temperature, Radiation Effects, and Corrosion Behaviour of Relevant Ni Alloys and Graphite"



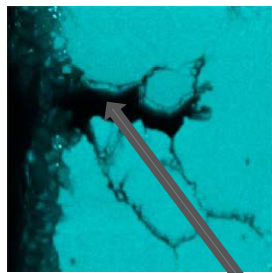
Combined environments Creep testing in molten salt



SEM

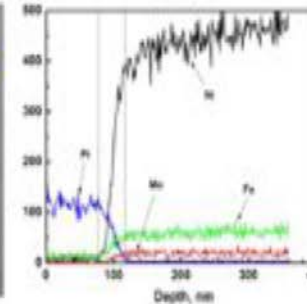
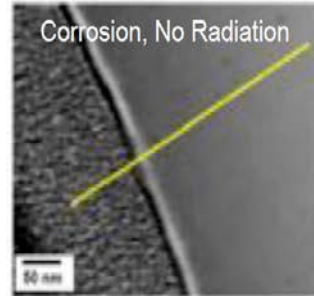
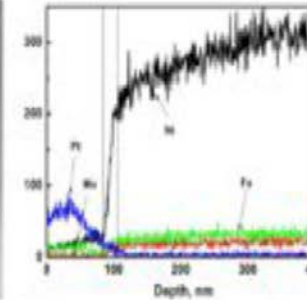
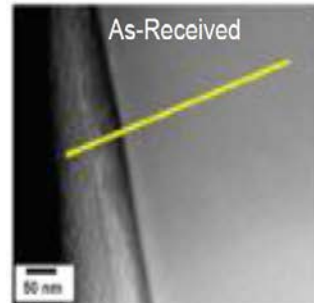


Euler Map

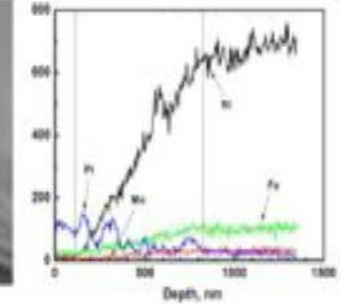
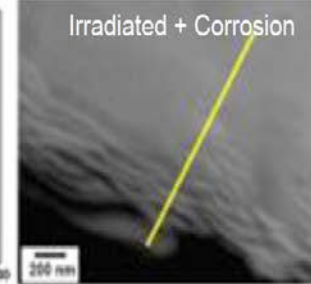
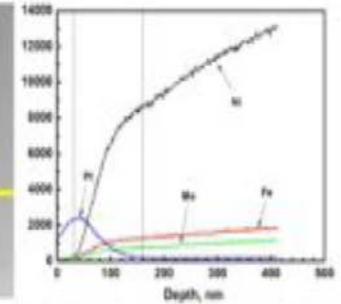
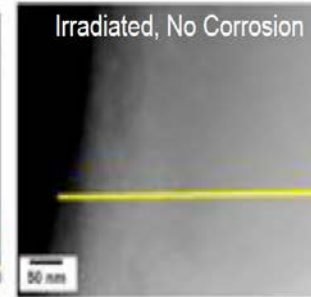


Cr

GH 3535 Creep testing in molten FLiNaK salt



Effect of Ion Irradiation on Corrosion



- GH3535 alloy, FLiNaK salt, 10^{17} ions/cm² He⁺
- He⁺ ion irradiation increases the thickness of the corrosion layer in the irradiated and corroded sample to more 30 times than in the un-irradiated sample

Evidence of preferential
grain boundary attack



Molten Salt Corrosion Loops at ORNL

Test loop	Structural material	Molten salt, % mole	Fluid test conditions				T _{alloy} °C	Corrosion rate µm/yr
			Circulation mode	T _{max} °C	Δ T _{max} °C	Exposure hrs		
NCL-1258	Stainless steel S-304L	70LiF-23BeF ₂ - 5ZrF ₄ -1UF ₄	Natural convection	688	100	6100	688	53
						79400	688	26
NCL-22	Stainless steel S-316	71.7LiF-16BeF ₂ - 12UF ₄ -0.3ThF ₄	Natural convection	650	110	4298	650	23
NCL-16	Hastelloy-N Hastelloy-N, mod. Ti≤0.5	66.5LiF-34BeF ₂ - 0.5UF ₄	Natural convection V=2.5cm/s	704	170	28000	660	1.0(1.0*)
							675	0.5
						700	0.9	
MSRE	Hastelloy -N	65LiF-29.1BeF ₂ -5.0-Zr F ₄ -0.9UF ₄	Fuel circuit circuit	654	22	21800	654	8.0(1,6*)
		66LiF-34BeF ₂	Coolant circuit	580	35	26100	580	no
NCL-15A	Hastelloy -N	73LiF-2BeF ₂ -5ThF ₄	Natural convection V=0.7cm/s	677	55	35400	677	1.5
NCL-21A	Hastelloy -N Hastelloy-N, mod. 1%Nb	71.7LiF-16BeF ₂ - 12ThF ₄ -0.3UF ₄	Natural convection V=1 cm/s U ⁴⁺ /U ³⁺ ≈10 ⁴	704	138	10009	704	3.5 (3.1*)
						1004	704	3.7
NCL-23	Inconel 601	71.7LiF-16BeF ₂ - 12ThF ₄ -0.3UF ₄	Natural convection V=1 cm/s, U ⁴⁺ /U ³⁺ ≈40	704	138	721	704	≥34
NCL-24	Hastelloy-N, mod. 3.4%Nb	68LiF-20 BeF- 11.7ThF-0.3UF ₄	Natural convection	704	138	1500	704	2.5
FCL-2b	Hastelloy -N Hastelloy-N mod. 1%Nb	71.7LiF-16BeF ₂ - 12ThF ₄ -0.3UF ₄	Forced convection V=2.5-5 m/s U ⁴⁺ /U ³⁺ ≈100	704	138	4309	704	2.6(2.5*)
						2242	704	0.4
FCL-2	Hastelloy -N	92NaBF ₄ -8NaF	V=2.3 m/s V=6.2 m/s	620	170	5100	620	12
						5100	620	16

* Calculated value for the diffusion-kinetic model

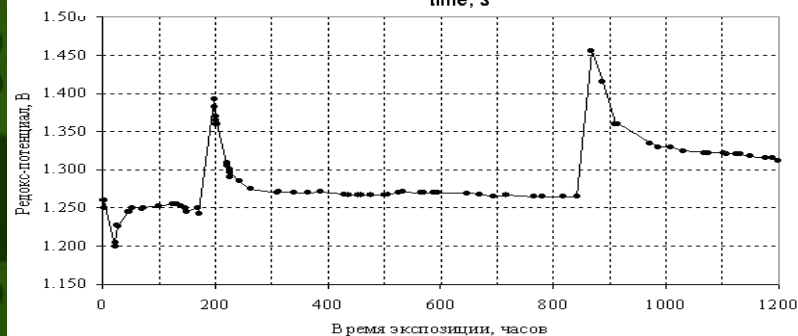
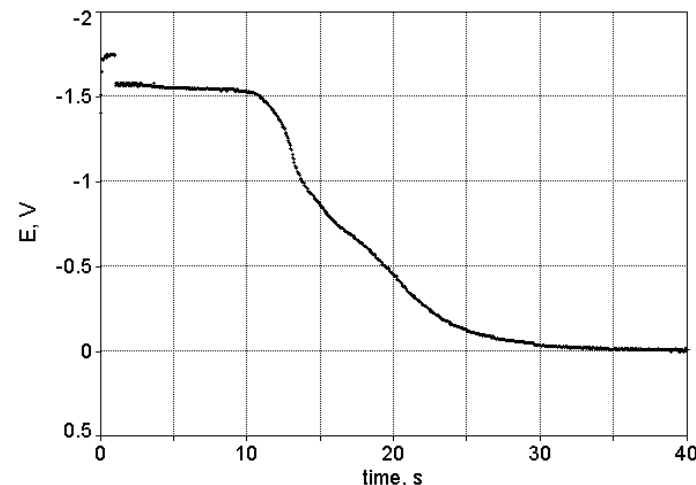
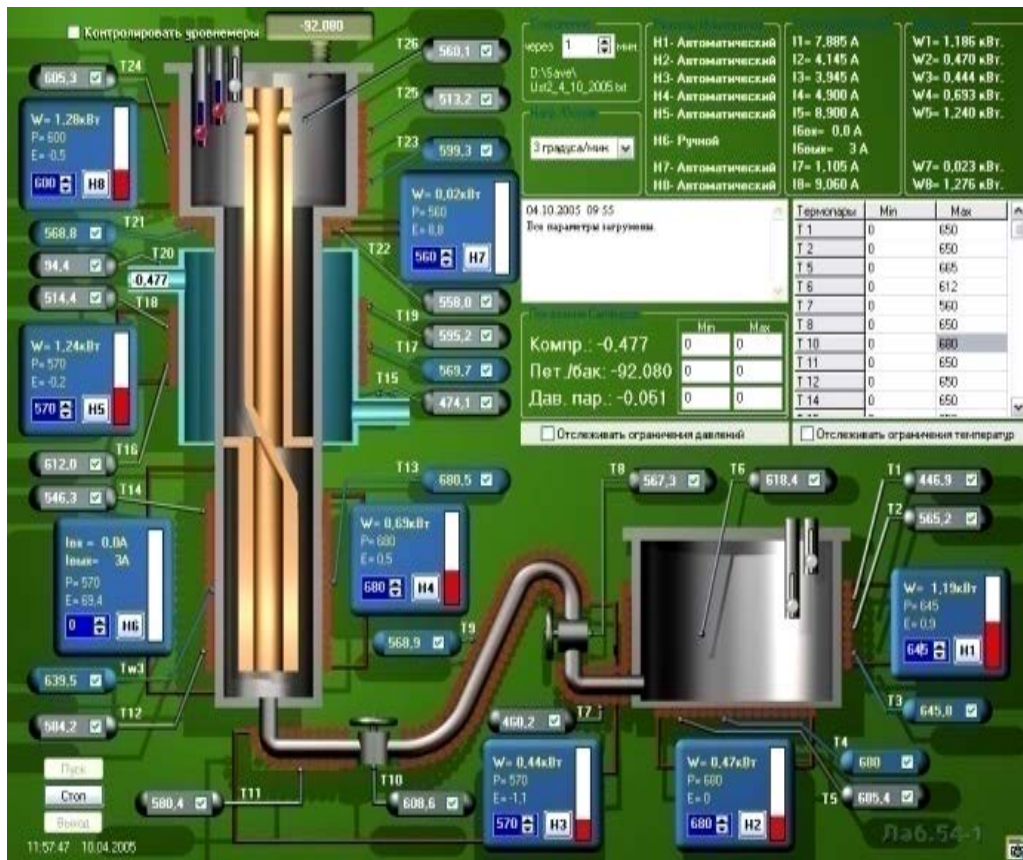


Molten Salt Corrosion Loops at KI

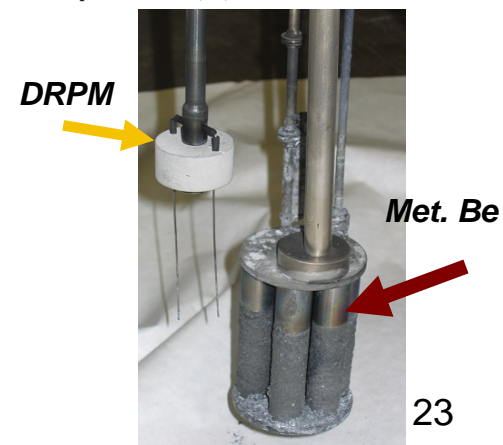
Loop	Salt, in mole %	Specimens material	T _{max} , °C	ΔT, °C	Exposure, hr	Corrosion rate, μm/yr
Solaris	46.5LiF-11.5NaF-42KF	12H18N10T HN80MT	620	20	3500	250 22
KI C1	92NaBF ₄ -8NaF	12X18H10T	630	100	1000	250
KI C2		AP - 164	630	100	1000	50
KI C3		HN80MT	630	100	1000	12
KI M1	66LiF- 34BeF ₂ +UF ₄	12H18N10T	630	100	500	20
KURS-2	66LiF -34BeF ₂ +UF ₄	12H18N10T	750	250	750	25
KI F1	71.7LiF-16BeF ₂ -12ThF ₄ -0.3UF ₄ +Te	HN80MT	750	70	1000	3.0
KI F2		HN80MTY	750	70	1000	6.0
NCL-1	15LiF-58NaF-27BeF ₂ +PuF ₃	HN80M-VI	700	100	1600	5
		HN80MTY				5
		MONICR				19
KI Te1	15LiF-58NaF-27BeF ₂ +Cr ₃ Te ₄	HN80M-VI	700	10	400	3
		HN80MTY				3
		MONICR				15
KI Te2	75LiF-5BeF ₂ -20ThF ₄ +2UF ₄ + Cr ₃ Te ₄ Average value [U(VI)/U(III)] = 5	HN80M-VI	730	40	250	29
		HN80MTY	735			57
		HN80MTW	735			28
		EM 721	735			10
KI Te3	73LiF -27BeF ₂ + 2.0UF ₄ +Te(metal) Average value [U(VI)/U(III)]= 45	Hastelloy N	760	40	256	21(20*)
		HN80MTY				8
		HN80MTW				12
	73LiF -27BeF ₂ + 2.0UF ₄ +Te(metal) Average value [U(VI)/U(III)]=85	EM 721	22			
		Hastelloy N	800	40	248	45(56*)
		HN80MTY	780			52
HN80MTW	800	63				
EM 721	800	55				



Li,Be,Na,Pu/F Thermal Convection Loop



It was developed three electrode design for measurement of redox potential with non-stationary dynamic beryllium reference electrode (DRPM). It is highly sensitive to variation of redox potential in molten BeF_2 - containing mixtures and ensures good reproducibility of measured values.





Two ways to get the required level of the salt purity were used:

1. To remove oxygen, nickel, and iron impurities
2. To refill the loop with fresh pure salt

Melt processing by gas mixture H_2+HF (ORNL)

reduce of oxidized forms of chromium, iron and nickel to Me

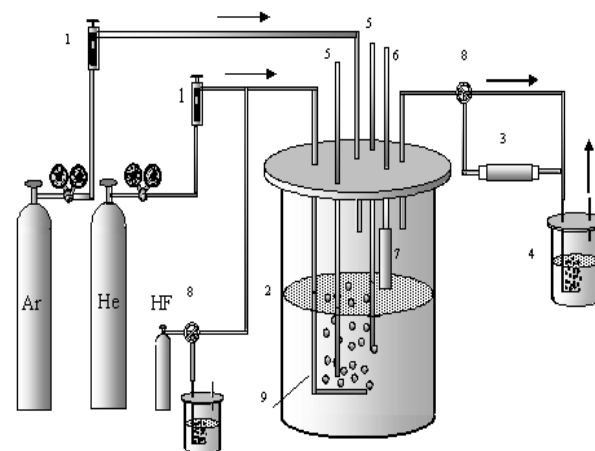
filtering the melt

Melt electrolysis

solubility of NiF_2 depends on oxygen concentration

necessary to remove oxygen

Fluorination without H_2



1 – rotameter, 2 – drain tank, 3 – humidity indicator, 4 – bubbler, 5 – graphite anode, 6 – gas removal line, 7 – metallic beryllium, 8 – valve, 9 – copper tube.

The following order of technological procedures of salt purification was chosen:

- Hydrofluorination of the melt by a mixture of hydrogen fluoride and helium in order to remove solid and dissolved oxides.
- Electrolysis of the salt melt aimed at removing the main amount of dissolved nickel.
- Processing of the salt melt by metallic beryllium in order to remove the rest of Ni and Fe.

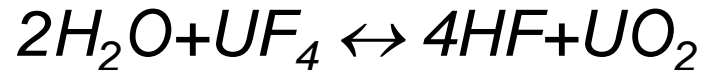
№	Procedure	Content of impurities, mass.%				The redox potential, V
		Ni	Fe	Cr	O	
1	Before purification	1,01	0,042	-	0,34	1,78
2	After 14 hours of HF-He processing 3 hours of He blowing at T = 580°C	0,57	0,047	-	< 0,08	1,95
3	After electrolysis (34 A·hr) plus helium blowing at T = 575°C	0,038	< 0,01	-	< 0,06	1,34
4	After 12 hours of processing by metallic beryllium at T = 580°C	0,0035	0,0127	0,007	< 0,06	1,38
5	Washing of a loop by melt. Repeated processing by metallic beryllium at T = 580°C	0,003	0,0165	0,0026	-	1,25



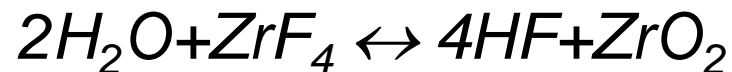
MSR Fuel Behavior

- Solubility has significance of impurities such as moisture react with molten salts to produce metal oxides of much higher melting point and correspondingly lower solubility.

For UF_4 fueled systems this reaction is written as:



- To prevent the loss of uranium from solution and possible accumulation of UO_2 precipitate in amounts large enough to pose criticality concerns, 5mole% of ZrF_4 was added to the solution of MSRE to getter any oxide impurities through the reaction:



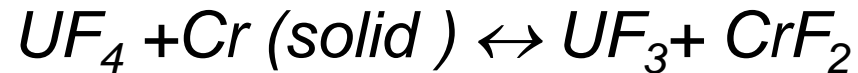
- Plutonium as PuF_3 shows little tendency to precipitate as oxide even in the presence of excess BeO and ThO_2



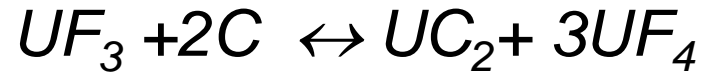
MSR Fuel Behavior

- Besides solubility concerns with respect to impurity reactions, one must prevent the liquid fuel component from reacting: with container or with moderator graphite.

Reactions of the former like as:



and the later:



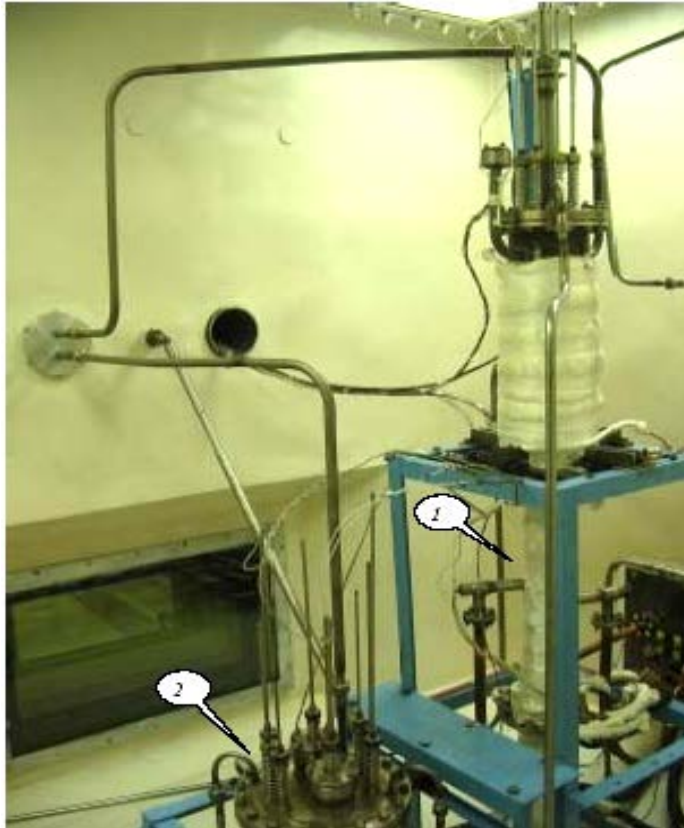
were prevented by careful control of the solution redox chemistry which was accomplished by setting the UF_4 / UF_3 ratio at approximately (50-60)/1.

- Additions of metallic Be to the fuel salt to effect the reduction of the UF_4 via:



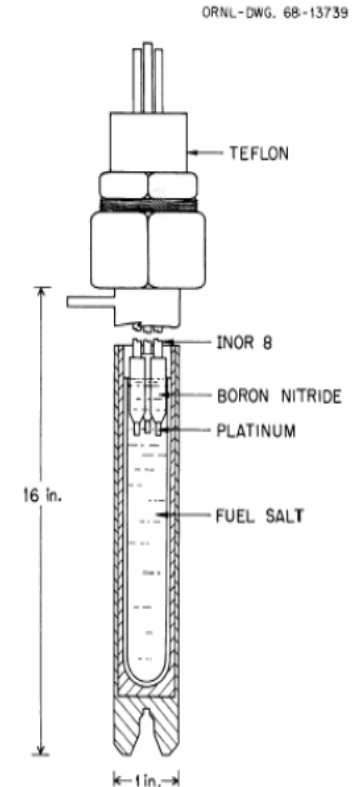
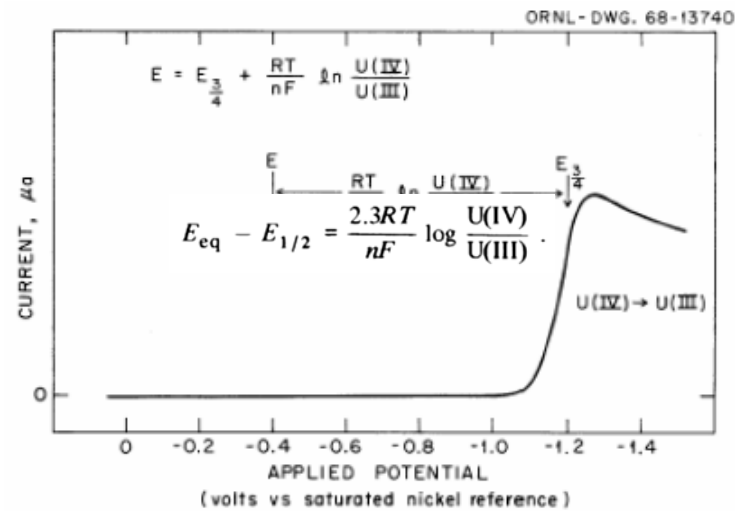


UF₄ Containing Corrosion Loops



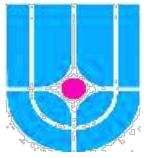
77.5LiF-20ThF₄-2.5UF₄+Te:

75LiF-20ThF₄ +5BeF₂+xUF₄+Te:

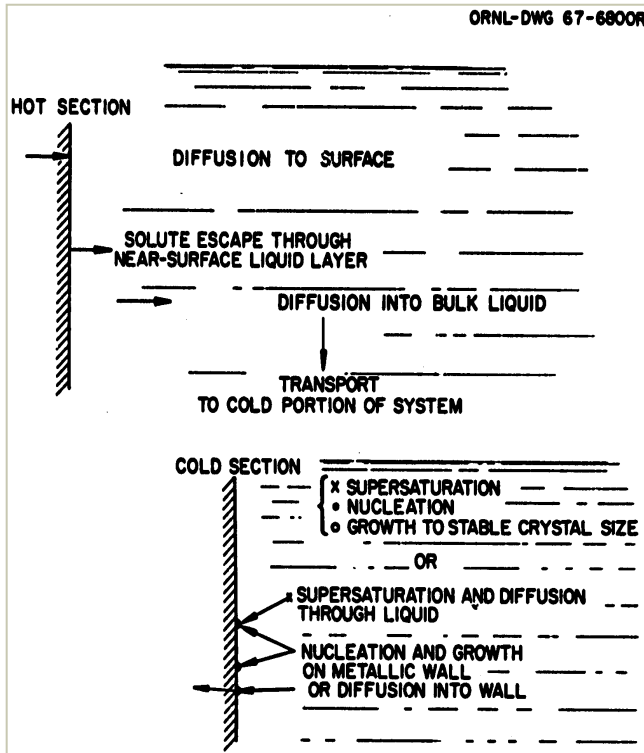


A simple voltammetric method was developed at ORNL for the determination of U(IV)/U(III) ratio. The method involves the measurement of the potential difference between the equilibrium potential of the melt, measured by an inert platinum electrode immersed in melt and voltammetric equivalent of the standard potential of the U(IV)/U(III) couple $E_{1/2}$.

For linear sweep voltammetry at a stationary electrode, the polarographic half-wave potential $E_{1/2}$ corresponds to the potential on voltammogram at which the current is equal to 85.2% of the peak current.



Temperature Gradient Mass Transfer



$$X_{Cr}F_2 = A_{Cr} (X_{UF_4}/X_{UF_3})^2 K(T)$$

X – component concentration

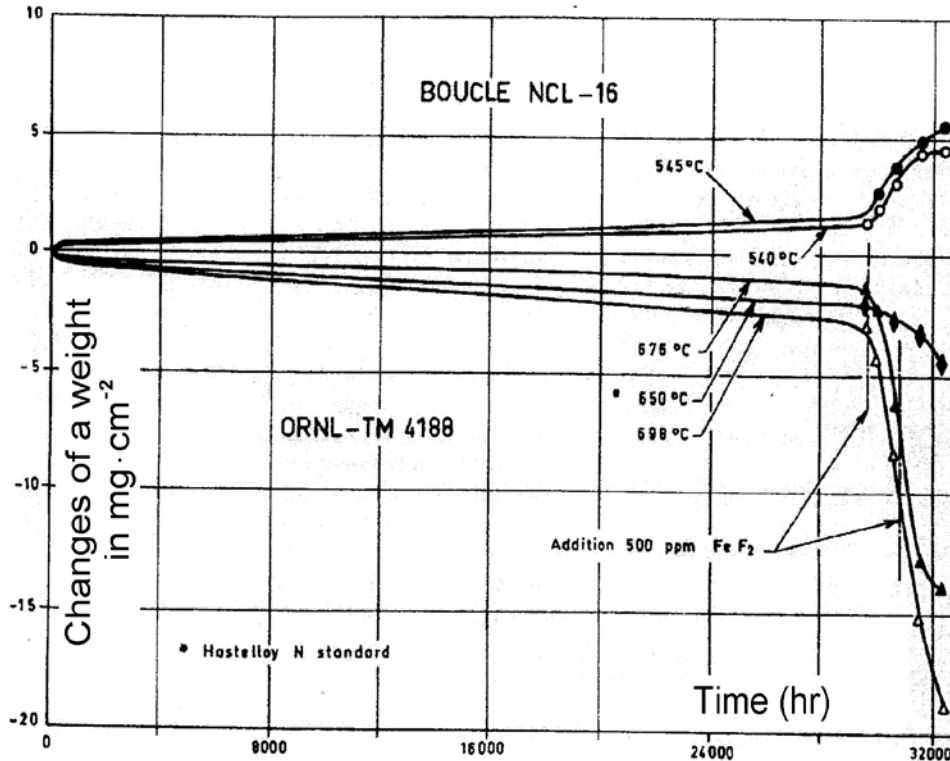
A_{Cr} – chromium activity in the metal solid solution

$K(T)$ – reaction constant

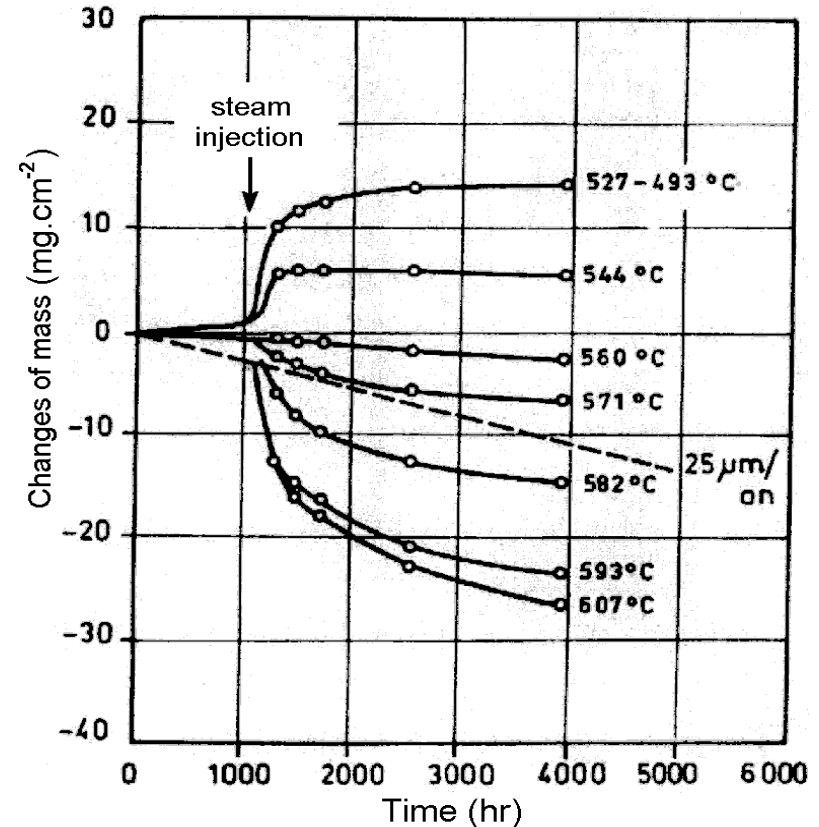
- The constant K depends on temperature
- In a large majority of cases, the metal tends to dissolve in the hot zone and metal deposition is observed in the cold zone
- In presence of a thermal gradient, equilibrium can be reached only by total consumption of the metal in the hot zone
- The slowest step of the process is usually ion transport in the liquid phase (by diffusion and convection)
- The corrosion rate depends on thermal gradient, but also on the concentration in solution of the transported species
- The oxidant content of the salt can therefore lead to much more serious consequences than predicted by calculations limited to isothermal conditions: oxidants accelerate the mass transfer under thermal gradient



Influence of impurities addition



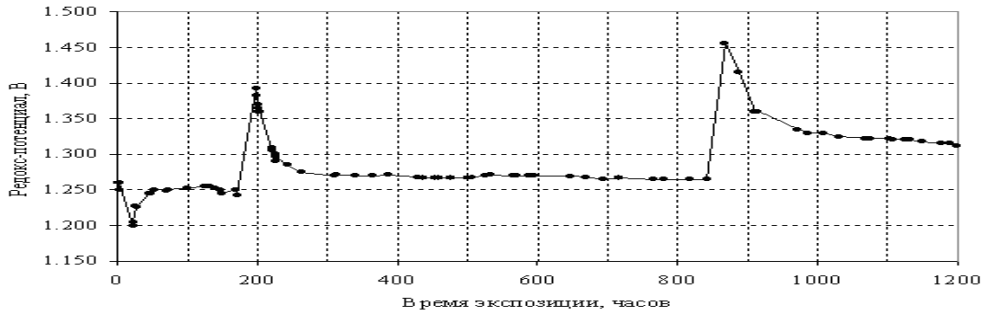
Influence of an addition of 500 ppm of FeF_2 on the corrosion behavior of a Hastelloy N loop containing a Li, Be, U/F



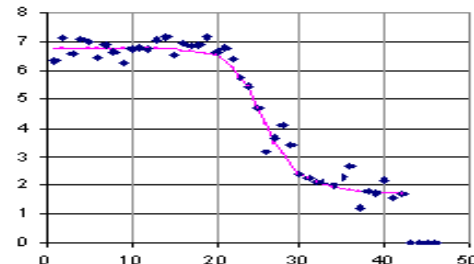
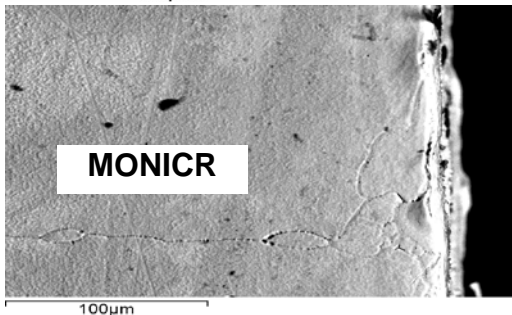
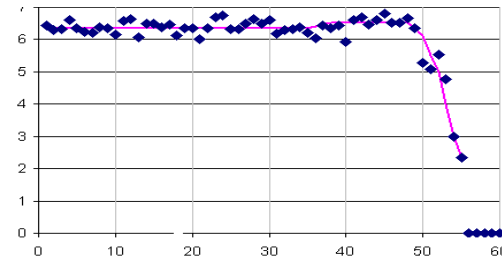
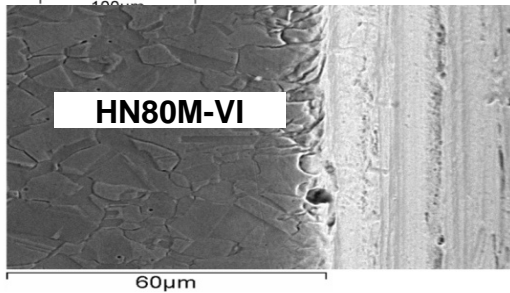
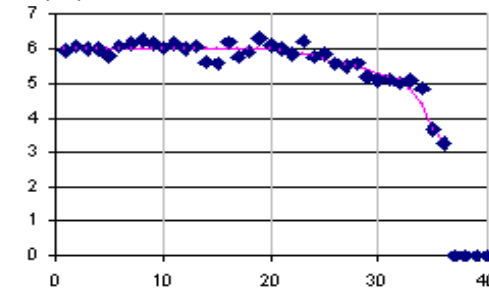
Influence of an water vapor injected in a NaBF_4 - NaF (92-8 mol%) mixture flowing in a Hastelloy N loop



Li,Be,Na,(Pu)/F Loop Corrosion Studies



- Results of 1200 hrs loop corrosion experiment with on-line redox potential measurement demonstrated that high temperature operations with molten $15\text{LiF}-58\text{NaF}-27\text{BeF}_2$ salt are feasible using carefully purified molten salts and loop internals.

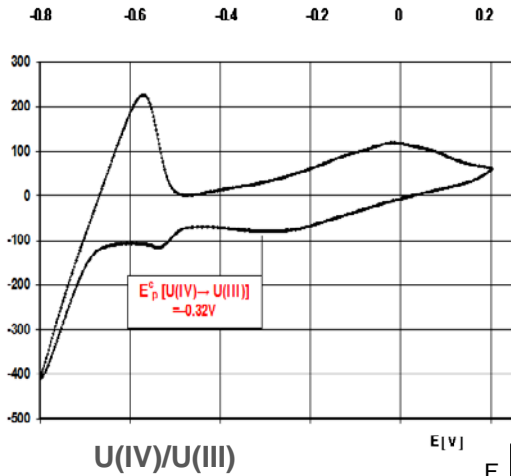


In established interval of salt redox potential 1.25-1.33 V relative to Be reference electrode, corrosion is characterized by uniform loss of weight from a surface of samples with low rate (2-5 $\mu\text{m}/\text{yr}$ for HN80M-VI and HN80MTY alloys and 9-19 $\mu\text{m}/\text{yr}$ for MONICR).

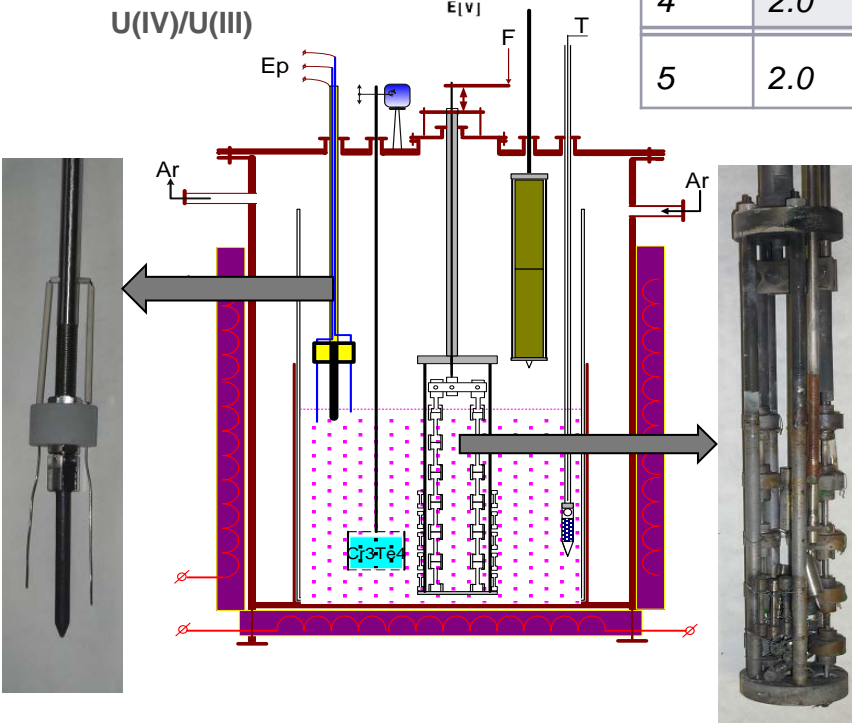
No intergranular corrosion of alloys is observed in the loop.



Te Corrosion in Li,Be,Th,U/F salt



Test	$[UF_3+UF_4]$ mole %	$[U(IV)]/$ $[U(III)]$	T °C	Impurity content in the fuel salt after test, wt. %				
				Ni	Cr	Fe	Cu	Te
1	0.64	0.7	735	0.0034	0.0018	0.054	0.002	0.015
2	2.1	4	735	0.0041	0.0019	0.006	0.0012	0.0032
3	2.1	20	735	0.009	0.0055	0.003	0.001	0.015
4	2.0	500	735	0.26	0.024	0.051	0.019	0.013
5	2.0	100	750	0.22	0.031	0.065	0.055	0.034



- The experimental facility was developed to study compatibility of Ni-based alloys under various mechanical loads to the materials specimens with fuel salts containing Cr_3Te_4 with redox potential measurement

- LiF-BeF₂-ThF₄-UF₄: 5 tests of 250 hrs each at fuel salt temperature till to 750°C and $[U(IV)]/[U(III)]$ ratio from 0.7 to 500

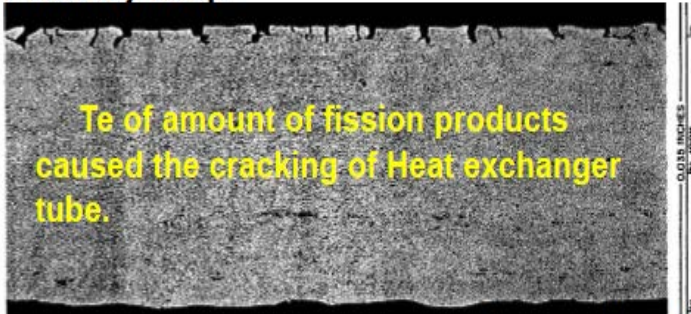
- LiF-BeF₂-UF₄: 3 tests of 250 hrs each at fuel salt temperature till to 800°C and $[U(IV)]/[U(III)]$ ratio from 30 to 90



N-alloys Compatibility With Fuel Salts Strongly Depends on Redox Potential

MSRE after 21000hrs

Primary loop



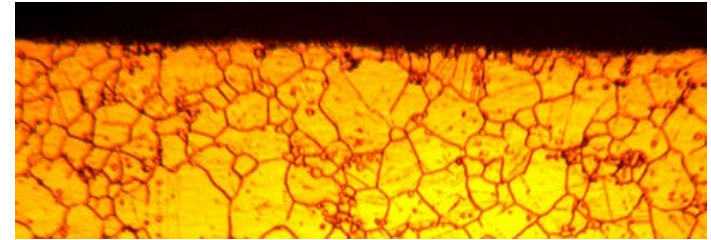
Secondary loop

Li, Be, U/F
U(IV)/(UIII)

Hastelloy N,
enlargement x160

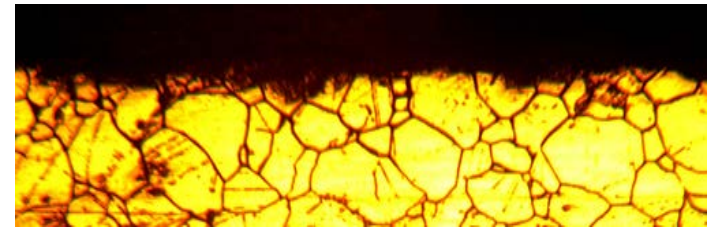
No

30
without
loading at
760°C



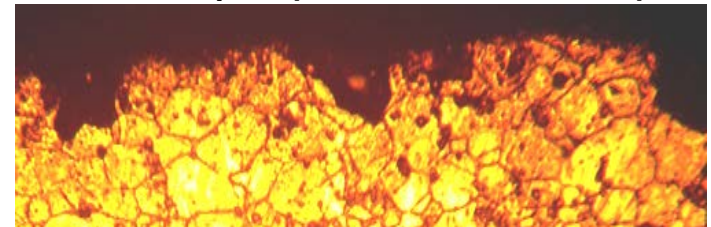
K = 3500pcxμm/cm ; l = 69μm

60
without
loading at
760°C

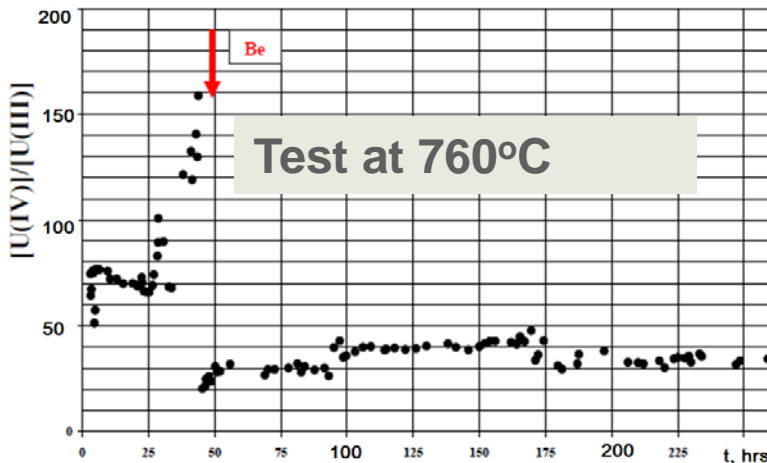


K = 4490pcxμm/cm ; l = 148μm

90
without
loading at
800°C

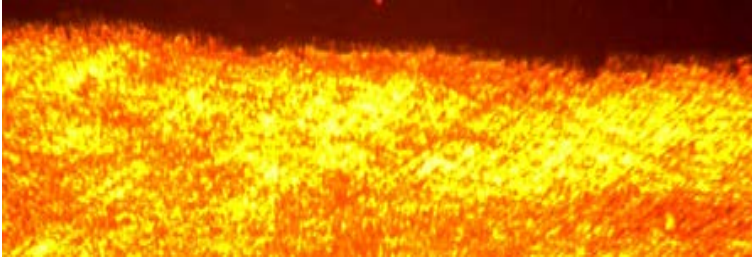
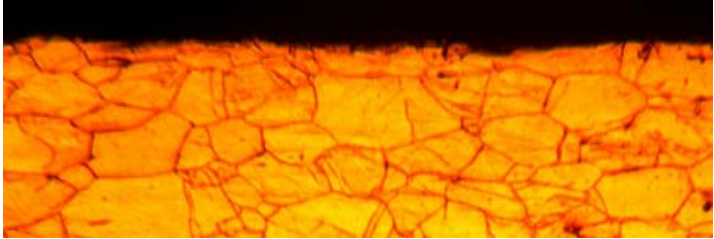
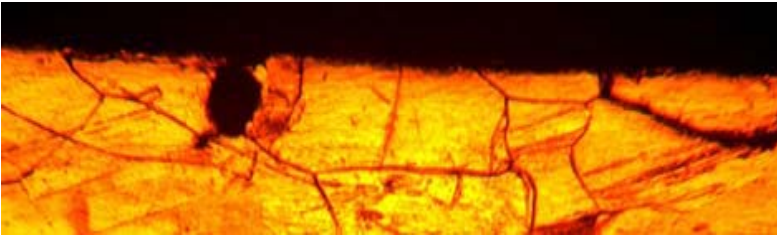
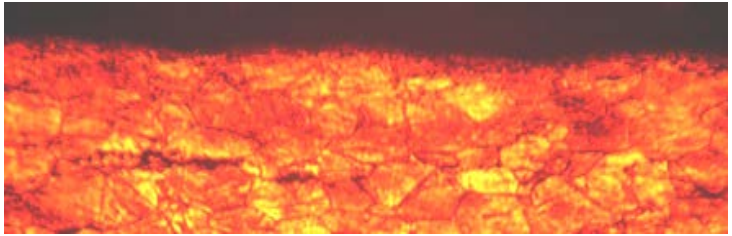
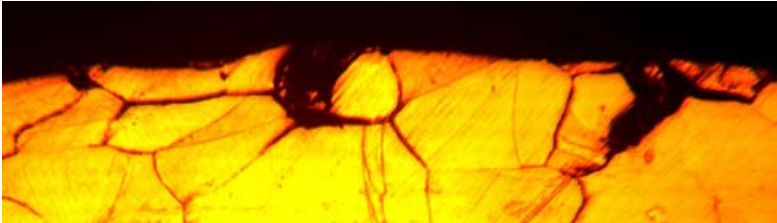
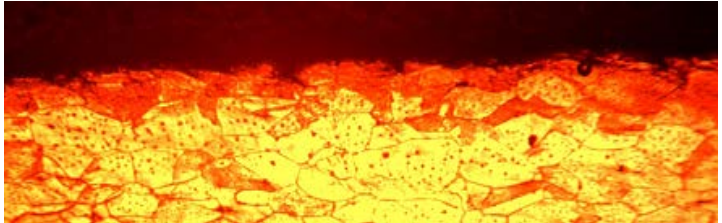


Decrease of RedOx potential by metallic Be



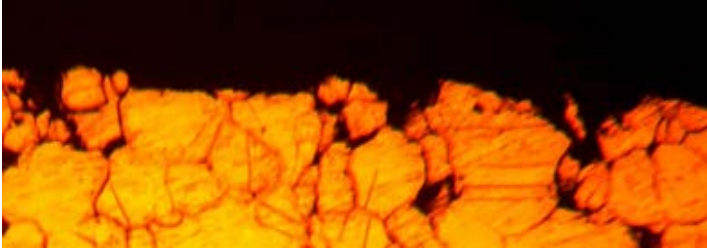
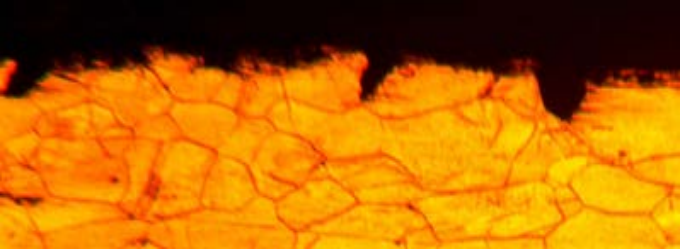
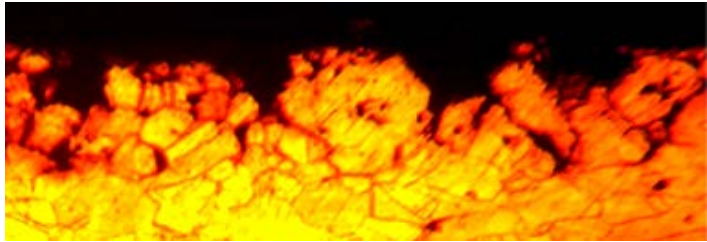
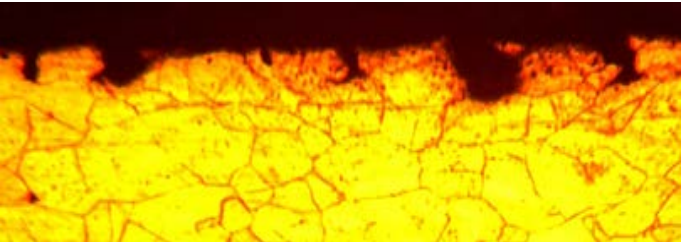
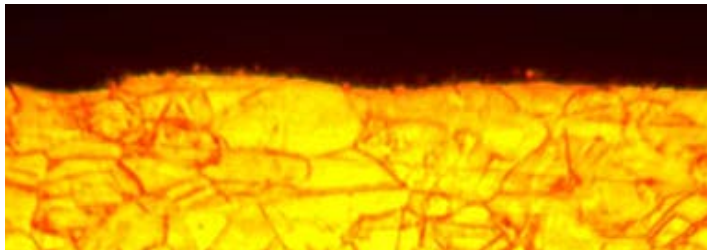
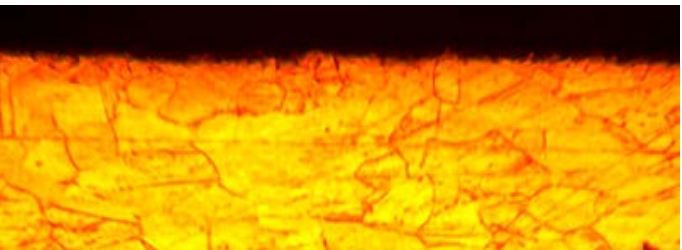


N-alloys Compatibility With Fuel Salts Strongly Depends on Redox Potential

$U(IV)/(U(III))$	EM-721, enlargement $\times 160$	HN80MTY, enlargement $\times 160$
30 without loading at 760°C	No 	No 
60 without loading at 760°C	$K = 3380pc \times \mu m/cm ; I = 117\mu m$ 	No 
90 without loading at 800°C	$K = 5830pc \times \mu m/cm ; I = 286\mu m$ 	$K = 530pc \times \mu m/cm ; I = 26\mu m$ 



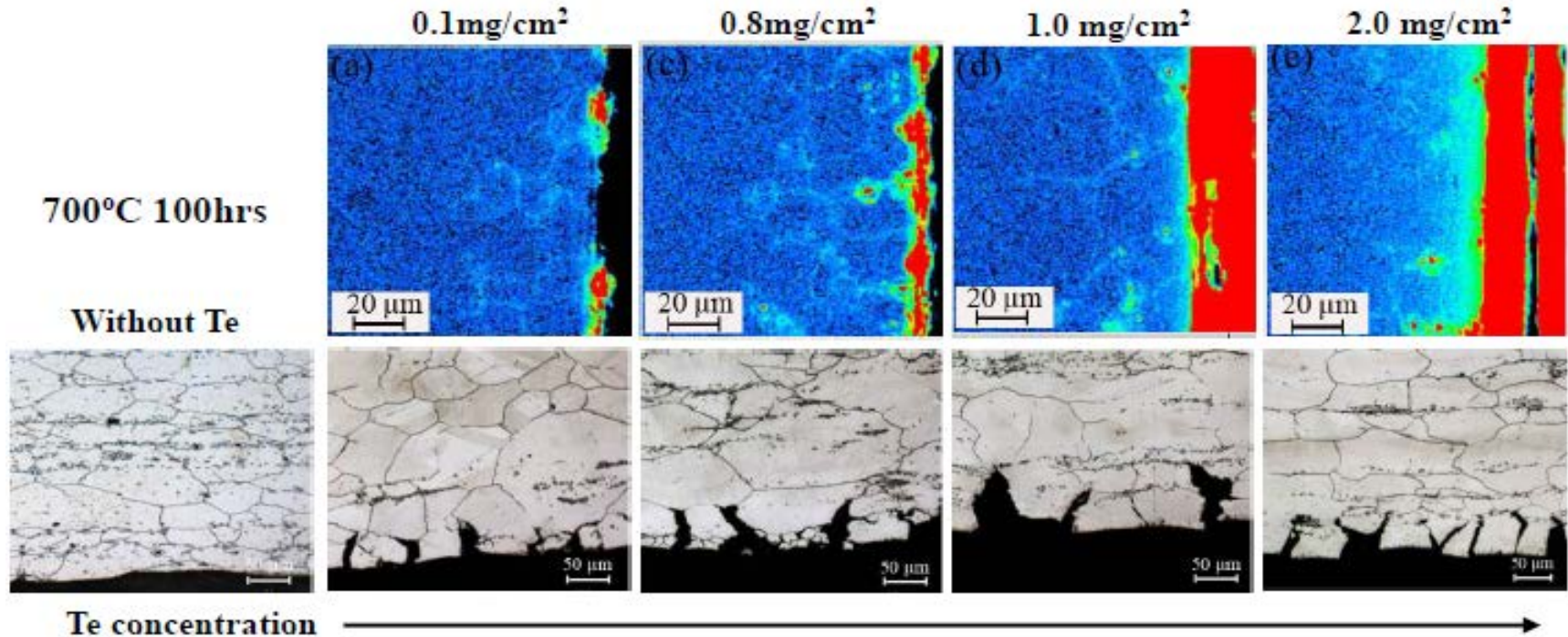
N-alloys Compatibility With Fuel Salts Strongly Depends on Redox Potential

<i>Li,Be,Th,U/F</i>	<i>HN80MT-VI</i>	<i>HN80MTY</i>
<i>[U(IV)]/[U(III)]</i> 500 <i>without</i> <i>loading at</i> <i>735°C</i>	<i>K = 3360pcxμm/cm; l = 166μm</i> 	<i>K = 1660pcxμm/cm; l = 68μm</i> 
<i>[U(IV)]/[U(III)]</i> 500 <i>Loading</i> <i>25MPa</i> <i>750°C</i>	<i>K = 8300pcxμm/cm; l = 180μm</i> 	<i>K = 1850pcxμm/cm ; l = 80μm</i> 
<i>[U(IV)]/[U(III)]</i> 100 <i>Loading</i> <i>25MPa</i> <i>750°C</i>	<i>no</i> 	<i>no</i> 



Characterization of Te IGC of alloy N

A typical molten salt experimental reactor running for 10 yrs, the Te content is 0.1 mg/cm^2
A typical molten salt demo reactor running for 10 yrs, the Te content 1.0 mg/cm^2



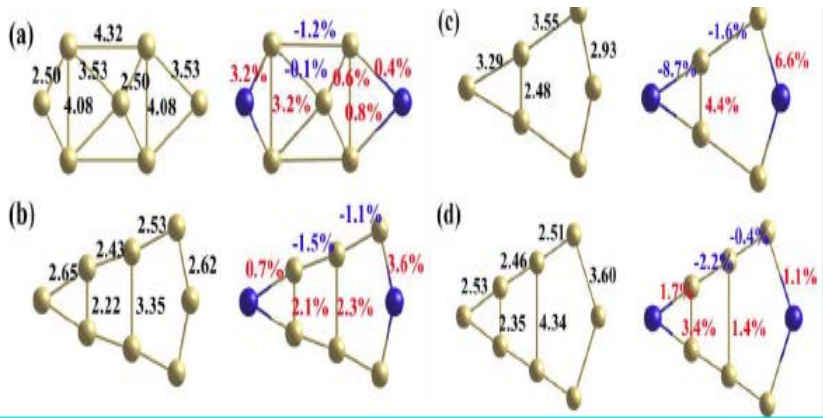
- Te content has greater impact on the reaction layer thickness and cracks width, but little affects the diffusion depth of Te in the alloy.
- Te diffuses into the alloy preferentially along the grain boundary at 700 C, which induces the decohesion and embrittlement of the grain boundaries and further deteriorate the mechanical properties of the alloy.

Te content didn't affect the diffusion depth, only results in the increase in reaction layer thickness



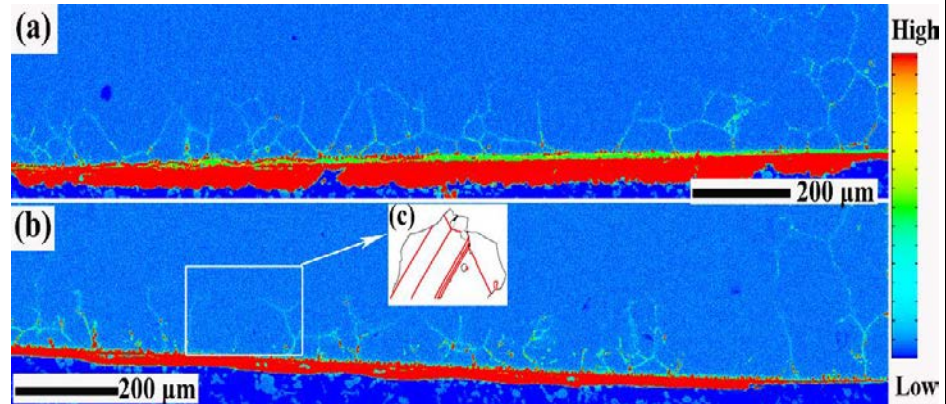
Effect of GBE on Te Diffusion in alloy N

Atomic structures of the clean GB(left) and Te-doped GB(right)



(a) $\Sigma=3(111)$, (b) $\Sigma=5(021)$, (c) $\Sigma=9(221)$, (d) $\Sigma=11(113)$

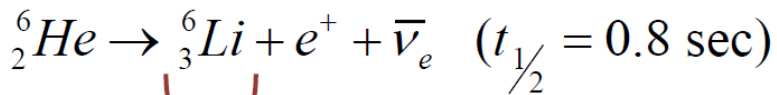
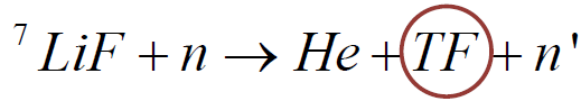
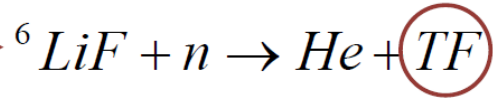
Element distribution mapping and diffusion depth of Te by EPMA in cross section of each sample exposed to Te vapor. (a) AR; (b) GBE; (c) the corresponding grain boundary character map of the GBE sample



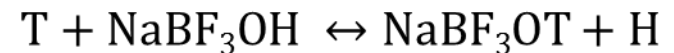
- Cr-Te presence at GBs and specifically at intergranular carbides/matrix interface, these brittle intermetallic compounds may ascribe to Te induced cracking.
- Tellurium diffuses in Alloy N mainly through GBs and prefer to transport along random high angle GBs than low Σ CSL GBs.
- Only $\Sigma 3$ boundaries have been found to be immune to Te penetration, and only such boundaries could be termed “special” grain boundaries in such case.
- From the cross section and the surface, the thinner corrosion layer and the fewer Te-attacked grain boundaries can be observed in the GBE sample.
- The improvement of resistance to Te diffusion in the GBE sample can be attributed to the large size grain-clusters associated with high proportion of the $\Sigma 3n$ boundaries.



Tritium Generation, Corrosion and Control Are Coupled. Can't Separate Tritium Generation, Corrosion and Control



After thermalization in fuel salt tritium is involved in chemical reactions:

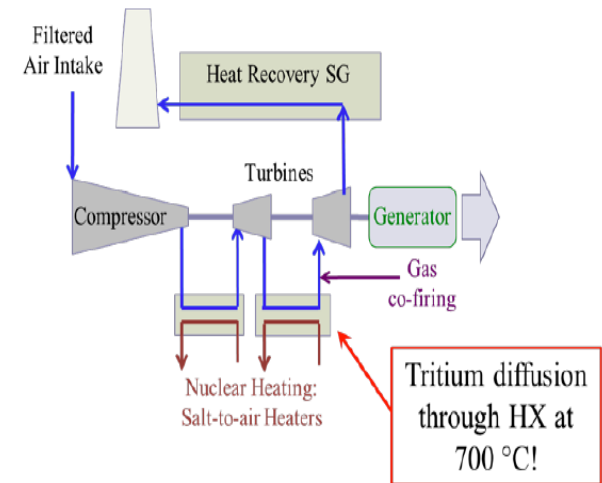


Corrosion - preferential attack of Cr in alloys by TF:

- $2\text{TF}(\text{d}) + \text{Cr}(\text{s}) \rightarrow \text{CrF}_2(\text{d}) + \text{T}_2(\text{g})$
- Corrosion reaction consumes TF, generates T_2

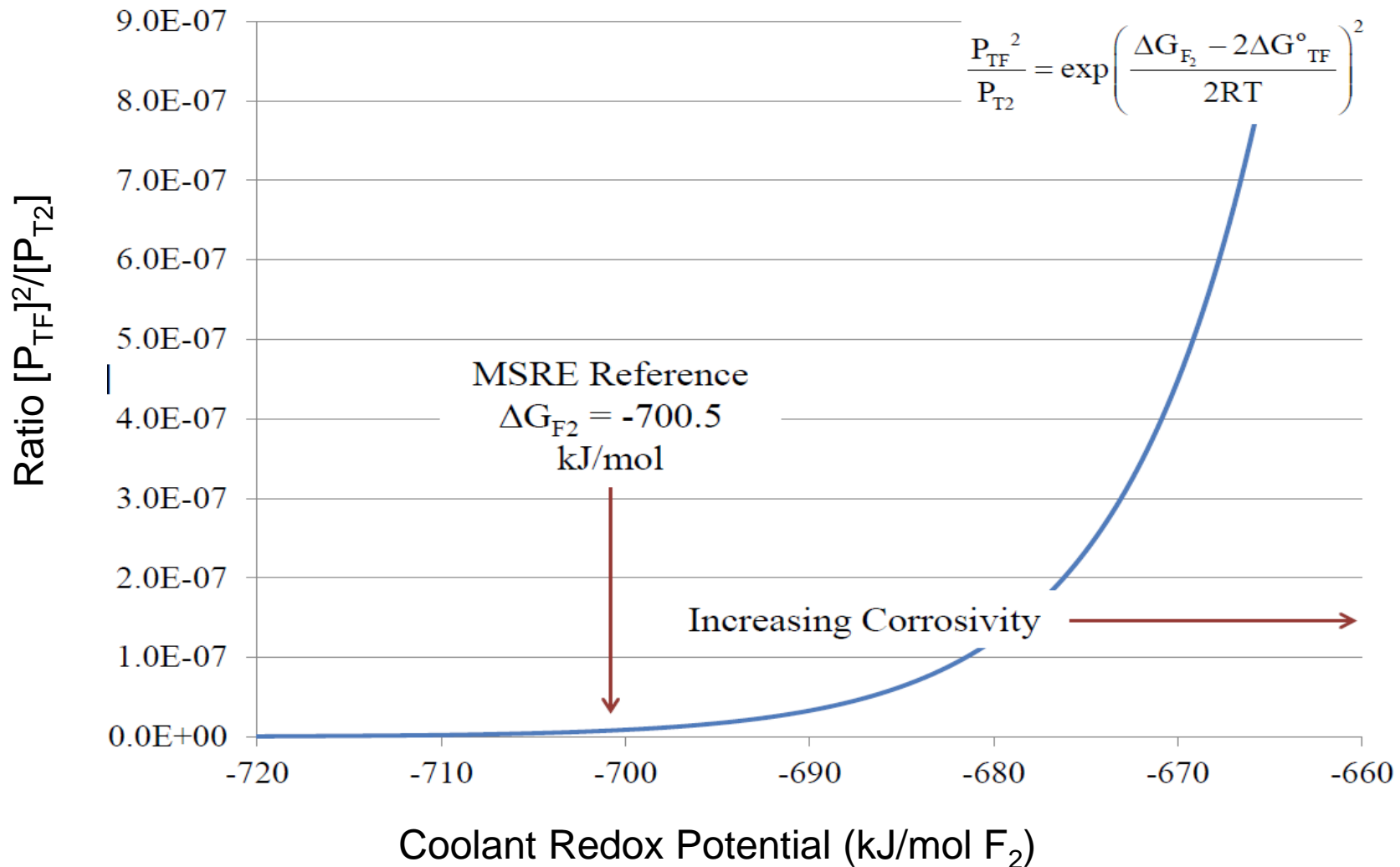
Radiological:

- T_2 fast diffusion through metal
- $T_{1/2} = 12.3 \text{ yr}$
- $\beta = 5.9 \text{ keV}$
- Must control corrosion and manage tritium escape from system





Redox Potential Dictates Relative Amounts of T₂ and TF



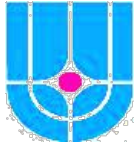


Tritium Control and Capture

Main strategies for mitigation include: advanced materials for the piping and heat exchangers, inert gas sparging, additional coolant lines and metal hydride addition or chemical removal

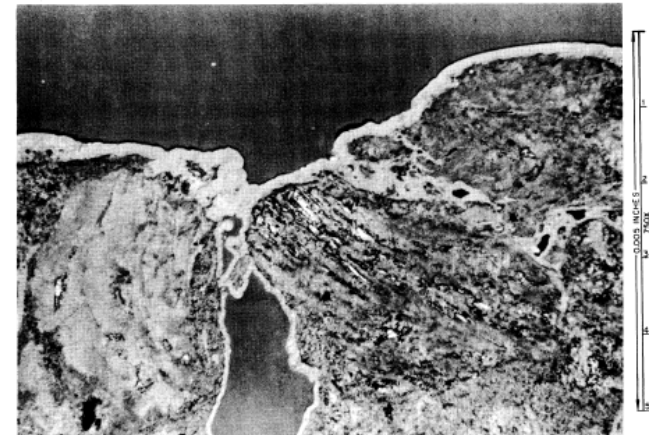
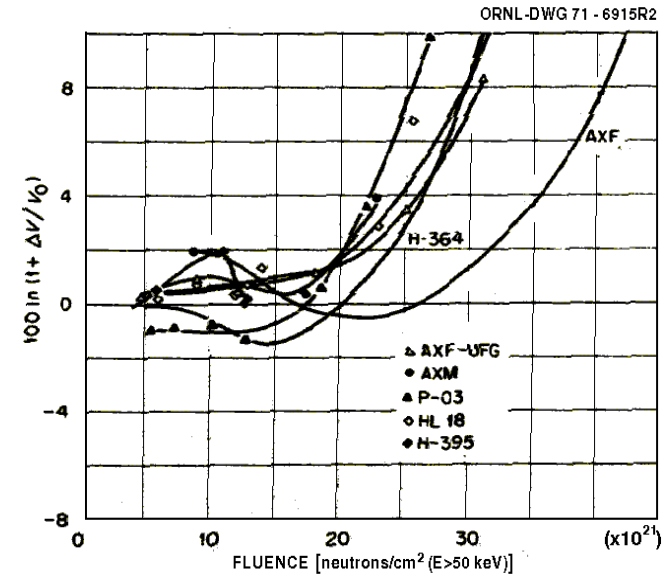
- *Additional development of permeation-resistant coatings, including W-Si*
- *Refinement of geometric configuration of the intermediate heat exchangers, minimizing tritium flux*
- *Discovery of reusable solvents for direct tritium removal from molten salt*
- *The chemistry of sodium fluoroborate and the trapping process by which tritium is retained by the salt*
- *Out-of-Core Tritium Removal with Carbon*

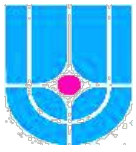
<i>Material</i>	<i>Temperature / Pressure</i>	<i>Equations Activation energy in kJ/mole</i>
<i>HN80MTY Mo-13,2%_{mass}</i>	<i>473...1123K 0.1...90 κPa</i>	<i>Diffusion $D=1,1 \cdot 10^{-7} \exp(-47,7/R \cdot T)$, [m² /s] Permeability $P=3,5 \cdot 10^{-8} \exp(-55,0/R \cdot T)$, [mole/m × s × Pa^{1/2}] Solubility $K_s=0.41 \cdot \exp(-8,85/R \cdot T)$ [mole/ m³ × Pa^{1/2}]</i>
<i>HN80MTY oxidation film</i>	<i>Same</i>	<i>Permeability $P=3,8 \cdot 10^{-8} \exp(-48,8/R \cdot T)$, [mole/m × s × Pa^{1/2}]</i>
<i>EM721 W-25,2%_{mass}</i>	<i>Same</i>	<i>Diffusion $D=4,5 \cdot 10^{-7} \exp(-45,7/R \cdot T)$, [m² /s] Permeability $P=3,7 \cdot 10^{-8} \exp(-55,4/R \cdot T)$, [mole/m × s × Pa^{1/2}] Solubility $K_s=0.13 \cdot \exp(-9,6/R \cdot T)$ [mole/ m³ × Pa^{1/2}]</i>
<i>77LiF-6ThF₄-17BeF₂ T_m =560°C (833K)</i>	<i>973-1073K 4-70 κPa</i>	<i>Diffusion $D=7,7 \cdot 10^{11} \exp(-393,5/R \cdot T)$, [m² /s] Permeability $P=1,5 \cdot 10^{-15} \exp(-38,8/R \cdot T)$, [mole/m × s × Pa^{1/2}] Solubility $K_s=2,0 \exp(-390,1/R \cdot T)$ [mole/ m³ × Pa^{1/2}]</i>



Graphite for MSR

- Graphite in a main part of MSR serves no structural purpose (its primary function is, of course, to provide neutron moderation) other than to define the flow patterns of the salt
- The requirements on the material are dictated most strongly by nuclear considerations, namely stability of the material against radiation induced distortion and non penetrability by the fuel bearing molten salt
- The main problems arise from the requirement of stability against radiation induced distortion
- The pyrolytic sealing work was only partially successful. Development of sealing techniques should be continuing



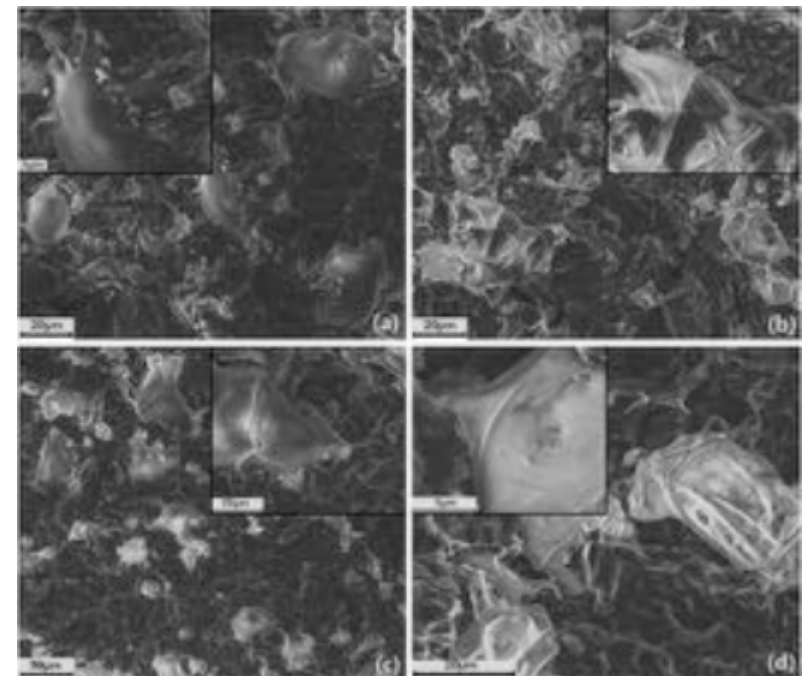


Production of Low Porous Nuclear Grade Graphite

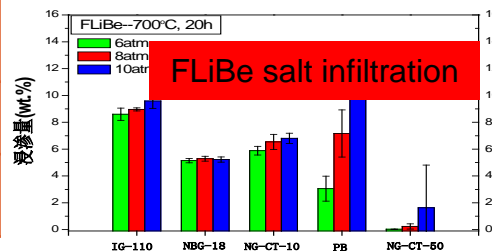
- Industrial production of ultrafine-grain nuclear graphite NG-CT-50
- Pore $< 1 \mu\text{m}$, ensured better FLiBe salt infiltration resistance than existing nuclear graphite
- Establishing performance database for NG-CT-50 graphite
- Participating in the international standards development of MSR graphite

Salt infiltration into various grades of graphite at different pressures (a) 1.0 atm; (b) 1.5 atm; (c) 3.0 atm; and (d) 5.0 atm.

Location of salt quantified via EDS (right) and neutron tomography (DINGO).



Parameters	NG-CT-50	IG-110
Pore Dia. mm	0.74	2
Boron ppm	< 0.05	0.1

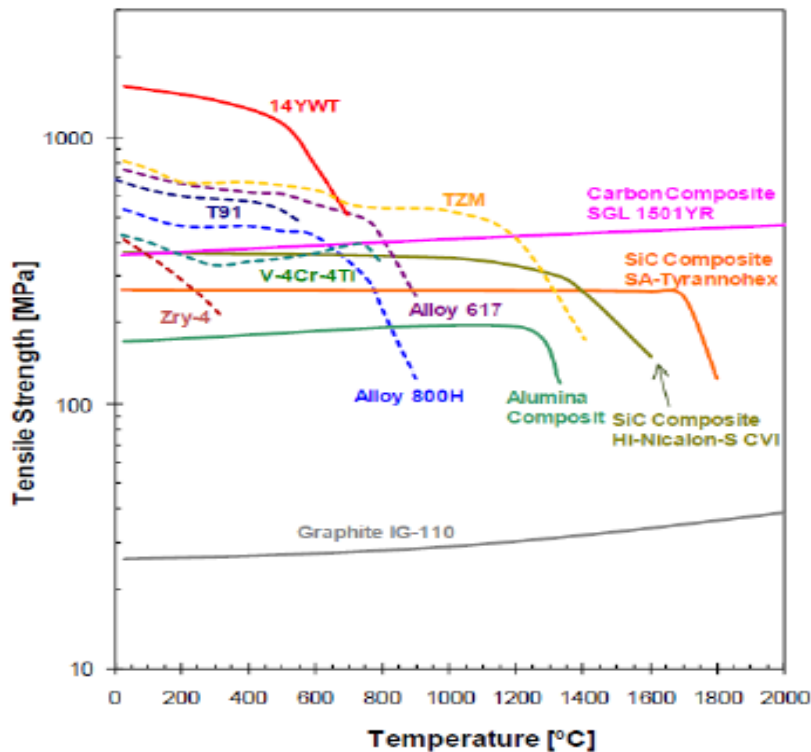




SiC-SiC and C-C Composites

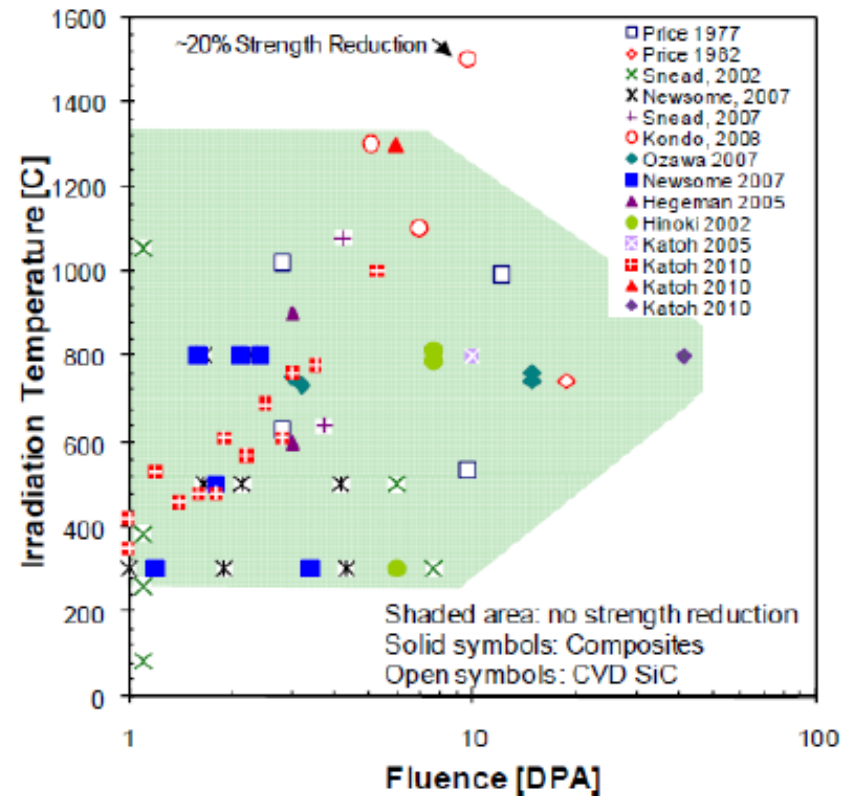
Advantages

Very good high temperature strength
 Low neutron absorption
 No radiation embrittlement



Challenges

Anisotropy effects
 Statistical failure
 Pseudo-ductile fracture -microcracking



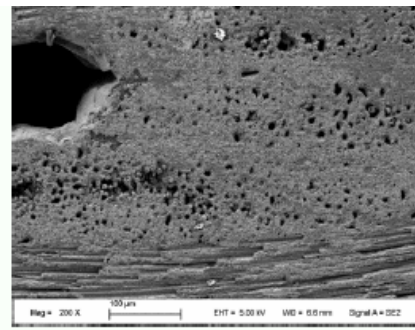
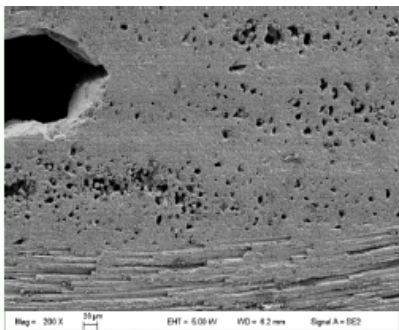
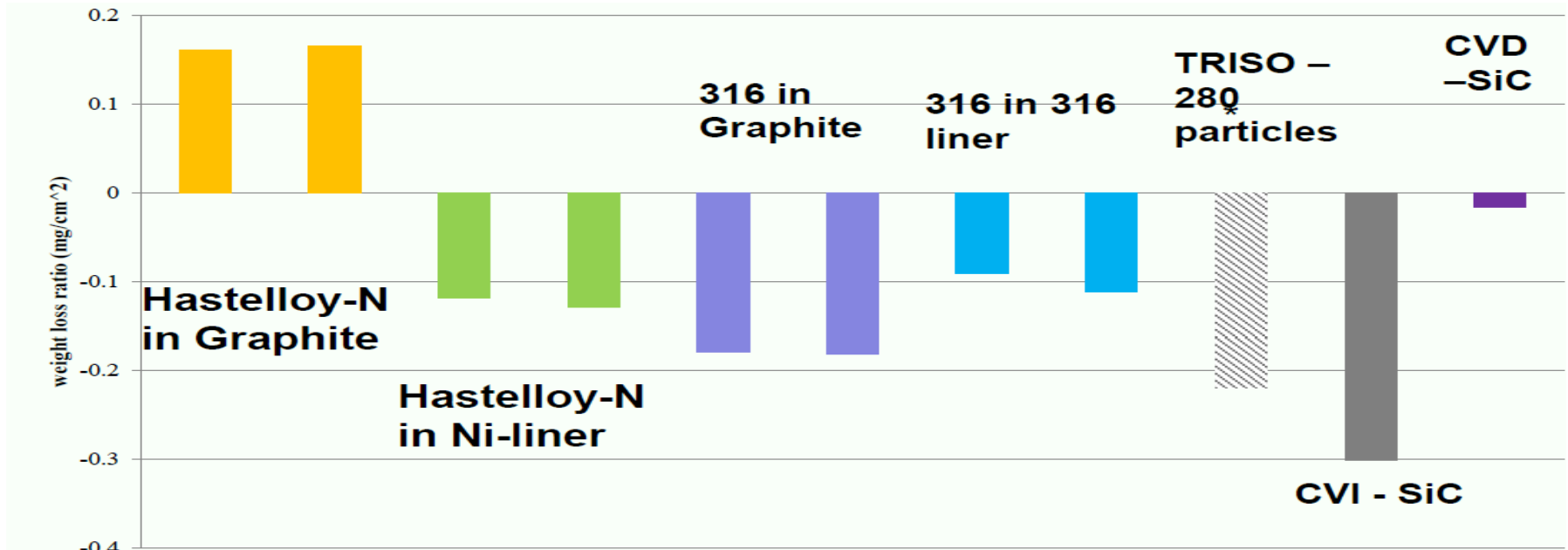


SiC-based materials have potential application in MSR due to its' low neutron-induced radioactivity, excellent irradiation tolerance, inherently low activation / low decay heat, and superior physical / chemical properties.

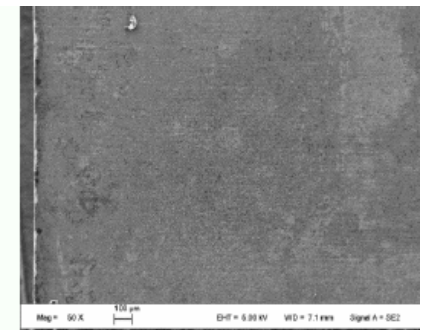
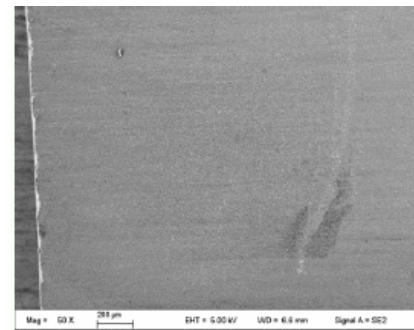
- The corrosion of CVD SiC, pressureless sintering SiC ceramic, SiC fiber and SiC_f/SiC composite in molten FLiNaK salt were studied.
- Results reveal that oxygen impurity in FLiNaK salt and SiC-based materials can both induce the corrosion.
- Hastelloy N alloy and its corrosion products can also affect the corrosion of SiC-based materials in molten FLiNaK salt.
- Ni in alloy can react with the corrosion product of SiC in salt to form nickel silicides (NiSi, Ni₃₁Si₁₂).
- NiF₂, the corrosion product of Ni, can result in the dissolution of SiC into salt as in the form of [SiF₆]²⁻. CrF₂ and CrF₃, the corrosion products of Cr, can react with SiC to form chromium carbides (CrC, Cr₃C₂, Cr₇C₃)



Corrosion of Composites in FLiBe



Tyranno-SA3 CVI SiC composite before (left) after (right) corrosion tests



CVD SiC composite before (left) after (right) corrosion test (negligible corrosion)



Fuel Processing Materials Development

- The materials requirements for MSR fuel processing systems are dependent upon the processing methods utilized and the design of particular equipment items selected for effecting these processing steps. Processes involving removal of uranium from fuel salt by fluorination and selective extraction of Pa and FPs products from fuel salt into liquid bismuth are considered the most promising method available, and the current processing materials studies is oriented in this direction.
- It is not necessary that a single material be compatible with all environments anticipated in the processing plant since the system can be designed to allow segregation of particular portions of the plant. It is expected that at least two classes of materials will be required: one for the fluorination and fuel reconstitution steps and another for the reductive extraction steps.
- Ni, which in some cases must be protected from corrosion by a layer of frozen salt, can be used for construction of fluorinators, and for those portions of a plant which contain fluorine, UF_6 and HF.
- Materials which have shown good compatibility with Bi solutions during limited tests include graphite and refractory metals such as tungsten, rhenium, molybdenum, and tantalum. Except for Ta, these materials are difficult to fabricate and join.



Summary

- Experience with the MSRE has proven the basic compatibility of the “graphite - Hastelloy-N - fluoride salt” system at elevated temperatures. However, a MOSART and MSFR will impose more stringent operating conditions, and some improvements in the Ni based alloy and probably graphite for this systems are needed.
- The mechanical properties of Hastelloy-N deteriorate under thermal-neutron irradiation, but the addition of titanium in combination with strong carbide formers such as niobium and hafnium makes the alloy more resistant to this type of irradiation damage.
- Graphite undergoes dimensional changes due to exposure to fast neutrons, and the possible loss of structural integrity due to these dimensional changes presently limits the lifetime of the reflector graphite. Studies to date indicate that graphite can be developed that have better resistance to irradiation damage than conventional nuclear graphites. The graphite used in the core will be sealed with pyrocarbon to reduce the amount of Xe that is absorbed. Techniques have been developed for this sealing, and studies are in progress to determine whether the low permeability is retained after irradiation.
- Corrosion studies indicate that the corrosion rate of Hastelloy-N in sodium fluoroborate is acceptable as long as the salt does not contain large amounts of impurities, such as HF and H₂O.